Bull. Soc. géol. Fr., 2007, t. 178, n° 6, pp. 437-458

Structural and metamorphic evolution of the Ambin massif (western Alps): toward a new alternative exhumation model for the Briançonnais domain

JEROME GANNE[1], JEAN-MICHEL BERTRAND[2], SERGE FUDRAL[3], DIDIER MARQUER[4] and OLIVIER VIDAL[5]

Key-words. – HP metamorphism, High-grade rocks exhumation, Crustal thinning, Flat-lying detachments, Western Alps, Penninic domain.

Abstract. – The basement domes of the central part of western Alps may result either from a multistage tectonic evolution with a dominant horizontal shortening component, an extensional behaviour, or both. The Ambin massif belongs to the "Briançonnais" domain and is located within the HP metamorphic zone. It was chosen for a reappraisal of the tectonic evolution of the Internal Alps in its western segment. Structural investigations have shown that Alpine HP rocks were exhumed in three successive stages. The D1 stage was roughly coeval with the observed peak metamorphic conditions and corresponds to a non-coaxial regime with dominant horizontal shortening and north movement direction. Petrological observations and P-T estimates show that the exhumation process was initiated during D1, the corresponding mechanism being still poorly understood. The D2 stage took place under low-blueschist facies conditions and culminated under greenschist facies conditions. It developed a retrogressive foliation and pervasive shear-zones at all scales that locally define major tectonic contacts. D2 shear zones show a top-to-east movement direction and correspond actually to large-scale detachment faults responsible for the juxtaposition of less metamorphic units above the Ambin basement and thus to a large part of the exhumation of HP rocks toward the surface. D2 shear zones were subsequently deformed by D3 open folds, large antiforms (e.g. the Ambin dome) and associated brittle-ductile D3 shear-bands. The D1 to D3 P-T conditions and P-T path of the blueschists occurring in the deepest part of the Ambin dome, was estimated by using the multi-equilibrium thermobarometric method of the Tweeq and Thermocalc softwares. Peak pressure conditions, estimated at about 14-16 Kb, 500ºC, are followed by a nearly-isothermal decompression that occurred concurrently with the major D1-D2 change in the ductile deformation regime. Eastwards, the Schistes Lustrés units exhibit a similar geometry on top of the Gran Paradiso dome but exhibit opposite D2 movement direction. Lower-grade units are lying above higher-grade units, the shear zones occurring in between being similar to Ambin's D2 detachments. Thus at regional scale, the D2 detachments seem to form together with the Ambin shear-zones, a network of conjugate detachments. Such a pattern suggests that the exhumation history is mostly controlled by a D2+D3 crustal-scale vertical shortening resulting in the thinning of the previous tectonic pile formed during D1. The slab-break off hypothesis may explain such an extensional behaviour within the western Pennine domain. It is suggested that the thermo-mechanical rebound of the residual European slab initiated between 35 and 32 Ma the fast exhumation of the previously thickened orogenic wedge (stack of D1 HP slices). It was immediately followed by a collapse of the wedge that may correspond to the E-W Oligocene extensional event responsible for the opening of rifts in the West European platform.

Évolution structurale et métamorphique du massif d'Ambin (Alpes occidentales) : nouvelles contraintes géodynamiques pour les modèles d'exhumation de type « Alpes »

Mots-clés. – Métamorphisme de HP, Exhumation de roches profondes, Amincissement crustal, Structure tectonique de détachement, Alpes occidentales, Domaine pennique.

Résumé. – Dans les Alpes occidentales, la plupart des modèles évolutifs envisagent que les nappes, formées de croûte océanique et de croûte continentale européenne et apulienne, ont été progressivement exhumées à la faveur d'une ou plusieurs phases tectoniques tangentielles syn-schistes bleus à vergence ouest ou nord-ouest, synthétiques de la subduction. Le problème abordé dans ce papier est celui de la dynamique d'exhumation de ces unités de nappes, métamorphisées à haute pression, que nous avons étudiées dans un secteur du domaine briançonnais – les Alpes Graies méridionales, en insistant surtout sur la traduction structurale et métamorphique des derniers stades de leur exhumation. Cette étude est centrée sur le dôme de socle Briançonnais du massif d'Ambin qui apparaît en fenêtre tectonique sous les couvertures océaniques des Schistes Lustrés.

Les principaux résultats de cette étude montrent : (1) qu'une phase tectonique syn-schistes bleus à vergence nord à nord-ouest est préservée. Mal exprimée dans les superstructures, elle est prédominante au cœur du dôme. Nous définissons ainsi un premier épisode D1 associé au pic de pression et de température (association grenat-jadéite – 15 Kb, 500 °C). (2) C'est une phase cisaillante post-HP à vergence est, l'épisode D2, qui est responsable de la structuration majeure du massif d'Ambin, tant dans les unités de socle que dans les unités de couverture. La déformation correspondant à cet épisode est syn-métamorphe depuis le faciès des Schistes bleus de bas grade (association glaucophane-chloritoïde:

1. Univ. Paul Sabatier, IRD / LMTG, 14 Avenue Edouard Belin, 31400 Toulouse, France. ganne@lmtg.obs-mip.fr
2. Univ. Savoie, Laboratoire de Géodynamique des Chaînes Alpines, 73376 Le Bourget-du-Lac, France
3. Univ. Savoie, EDYTEM, 73376 Le Bourget-du-Lac, France
4. Univ. Franche-Comté, Departement des Géosciences, 16 route de Gray, 25030 Besançon, France
5. Univ. Joseph Fourier, Laboratoire de Géodynamique des Chaînes Alpines, 1381 rue de la Piscine, 38400 St-Martin d'Hères, France.
Manuscrit déposé le 20 décembre 2006; accepté après révision le 15 mai 2007

7 à 9 Kb, 480°C) jusqu'au faciès des Schistes verts (association chlorite-albite: 3 à 5 Kb, 300 °C). (3) A une échelle plus régionale, nous montrons que les zones de cisaillement D2 post HP à vergence est (décrites dans les massifs d'Ambin et Vanoise Sud), Ouest (décrites à l'ouest des massifs du Gran Paradiso et de Dora Maïra) ainsi que les cisaillements à vergence conjuguée (décrits dans l'ensellement des Schistes Lustrés situé entre ces massifs) s'inscrivent globalement dans un mécanisme de déformation par amincissement, qui contribuent à une part importante de l'exhumation des roches alpines de HP-BT. Dans le scénario proposé, l'amincissement D2 survient à la limite Eocène supérieur – Oligocène inférieur, à la suite d'une perturbation thermique et mécanique affectant la lithosphère européenne (rupture du panneau lithosphérique plongeant ?). Cet épisode d'amincissement D2 marque donc une frontière géodynamique majeure entre l'histoire ductile des domaines internes (dynamique précoce de type subduction liée à l'exhumation des unités HP) et l'histoire de la collision post-oligocène qui prédomine dans les domaines externes (dynamique tardive de type collision associée au fonctionnement des bassins molassiques d'avant chaîne).

INTRODUCTION

High pressure – low temperature (HP-LT) metamorphic conditions are achieved during the deep burial of rocks either by subduction or by thickening of the crust [Platt, 1993]. The subsequent return of well-preserved metamorphic assemblages to the Earth's surface in active convergent zones, must imply fast exhumation processes [Rubatto and Hermann, 2001]. As HP-LT metamorphic rocks occur in various tectonic contexts (internal part of collisional belt, melange zones in accretionary prism, oblique subduction….) and display different tectono-metamorphic evolutions [Cloos, 1982; Spalla *et al.,* 1996], several mechanisms may be involved during their exhumation. Several models have been proposed to explain fast exhumation [see a review in Platt, 1993]. It is then critical to get precise geological information to propose robust structural constraints to explain exhumation processes. In the Alpine belt, the Ambin massif was chosen as a case study because it corresponds to an almost perfect basement dome that preserves HP-LT metamorphic assemblages. The Ambin massif occupies a key position among the metamorphic units of the Internal western Alps (Briançonnais and Piemont domains). Close to UHP units of the Piemont domain (e.g. Dora Maira massif, fig. 1A), it represents with the Acceglio zone and South Vanoise massif the most Internal Briançonnais unit. The aim of this paper is to discuss metamorphic P-T conditions together with new structural observations and their consequences on the knowledge of exhumation processes. A comparison with literature data and new observations from neighbouring HP-LT units (Gran Paradiso and "Schistes Lustrés") leads to propose a tentative model for the exhumation of Alpine HP-rock and the formation of the dome structures in the Briançonnais (Penninic) domain. We will especially insist on the events that occurred after the subduction and the initial HP stages of exhumation, i.e. those corresponding to retrograde metamorphic conditions.

GEOLOGICAL SETTING

The main units of the western Alps (fig.1A) are distinguished from west to east: the external units of the Dauphiné (or Helvetic), the lower Penninic units of the Valais together with Briançonnais and sub-Briançonnais, and finally the upper Penninic units: Piemont (internal crystalline massifs), Liguria-Piemont "Schistes Lustrés" (oceanic sutures) and Austro-Alpine units. The Ambin forms a dome-shaped basement window (fig. 1) beneath allochthonous metamorphic envelopes of various origins (Briançonnais Mesozoic margin-derived units, Liguria-Piemont zone ocean-derived units). Almost parallel envelopes define the dome. Structural discontinuities separate lithological groups previously defined by Gay [1971]. They are, from bottom to top: 1) The Claréa and Ambin Groups forming the pre-Permian basement; 2) The Permo-Triassic Etache Group and overlying metasediments of Triassic to Eocene age; 3) The "Schistes Lustrés", Jurassic to Cretaceous allochthonous metasediments of the Liguria-Piemont zone. The sketch sequence illustrated on figure 1B was drawn from the literature and available maps [Fudral *et al.,* 1994; Polino *et al.,* 1999].

To simplify the reading of this article, we have limited ourselves to presenting only the essential sedimentological and petro-metamorphic data from the Ambin Briançonnais basement and adjacent Schistes Lustrés units. The reader can easily refer to previously published articles [Ganne *et al.,* 2003, 2005, 2006; Chalot-Prat *et al*., 2003 for the Schistes Lustrés] for more extensive descriptions of the structures recognized in the Ambin and South Vanoise massifs. A complete database is also available at the following web address: (*http://tel.ccsd.cnrs.fr/documents/archives0/00/00/67/68/index_fr.html*).

The structurally deepest Claréa Group was interpreted for long as a polymetamorphic basement [Borghi *et al*., 1999 and reference therein] and the overlying Ambin Group was previously attributed to a Permian unconformable cover [Gay, 1971].

The ***Claréa Group*** is constituted by banded micaschists. Average mineral composition comprises: phengitic white micas, quartz, albite, glaucophane, chlorite, ± biotite, ± epidote, ± garnet, ± chloritoid, ± calcite, + accessory minerals [Michel, 1957; Gay, 1971]. Fine-grained amphibolites, composed of green hornblende, epidote, albite, titanite and rutile, also occur, associated with blueschists and greenschists (glaucophane + chlorite) and with rare marbles. Such rocks probably derive from a pelitic, flysch-type sequence with some mafic horizons [Gay, 1971; Pognante *et al.,* 1984; Polino *et al.,* 1999]. The presence of Variscan relics in the Claréa Group was assumed from the occurrence of garnet, large biotite and staurolite pseudomorphs [Bocquet, 1974; Borghi *et al*., 1999; Desmons *et al.,* 1999]. A ^{39}Ar-^{40}Ar biotite age of 340 Ma supports this hypothesis [Monié, 1990].

The ***Ambin Group*** is formed by several arenaceous sequences that comprise metaconglomerates. It shows also phengite-rich micaschists with rare greenschist and blueschist horizons, felsic layers, arkosic or rhyolitic in origin, and lenses of metadolomites or marbles. Three superimposed lithological units (A, B, C) are sketched on figure 1B.

– Unit A comprises phyllonitic rocks where isolated quartz pebbles may derive from metaconglomerates/metagreywackes. West of the massif the contact between the Claréa and Ambin Groups corresponds to a thick (> 10 m) shear zone that occurs at the base of unit A whereas eastwards, the shear zone is more diffuse (fig. 2).

– Units B and C correspond to several sedimentary sequences where well-preserved metaconglomerates/metagreywackes are grading upward to light green micaschists and associated calcite-ankerite calcschists.

– Unit C contains thin greenschist layers that grade eastwards to a thick cap of greenschists, metagabbros and metarhyolites (lower Claréa valley and Exilles-Ramats area – Polino *et al.* [1999]). Metarhyolites yielded ca. 500 Ma U-Pb on zircon ages [Bertrand *et al.,* 2000].

The ***Etache Group*** overlies the basement (unit D on figure 1B, figure 2) and shows a recurrent trilogy (phengite schists, green quartzites and calcschists) that grades upward to phengite-rich quartzites with sporadic pink quartz grains. The contact between Ambin and Etache groups is always outlined by a conspicuous increase in the deformation intensity (concentration of shear bands) that is interpreted as resulting from a major shear zone.

Above the Etache Group ***sedimentary Briançonnais formations*** include white Scythian quartzites and Jurassic to Cenozoic formations (unit E on fig. 1B, fig. 2) that form

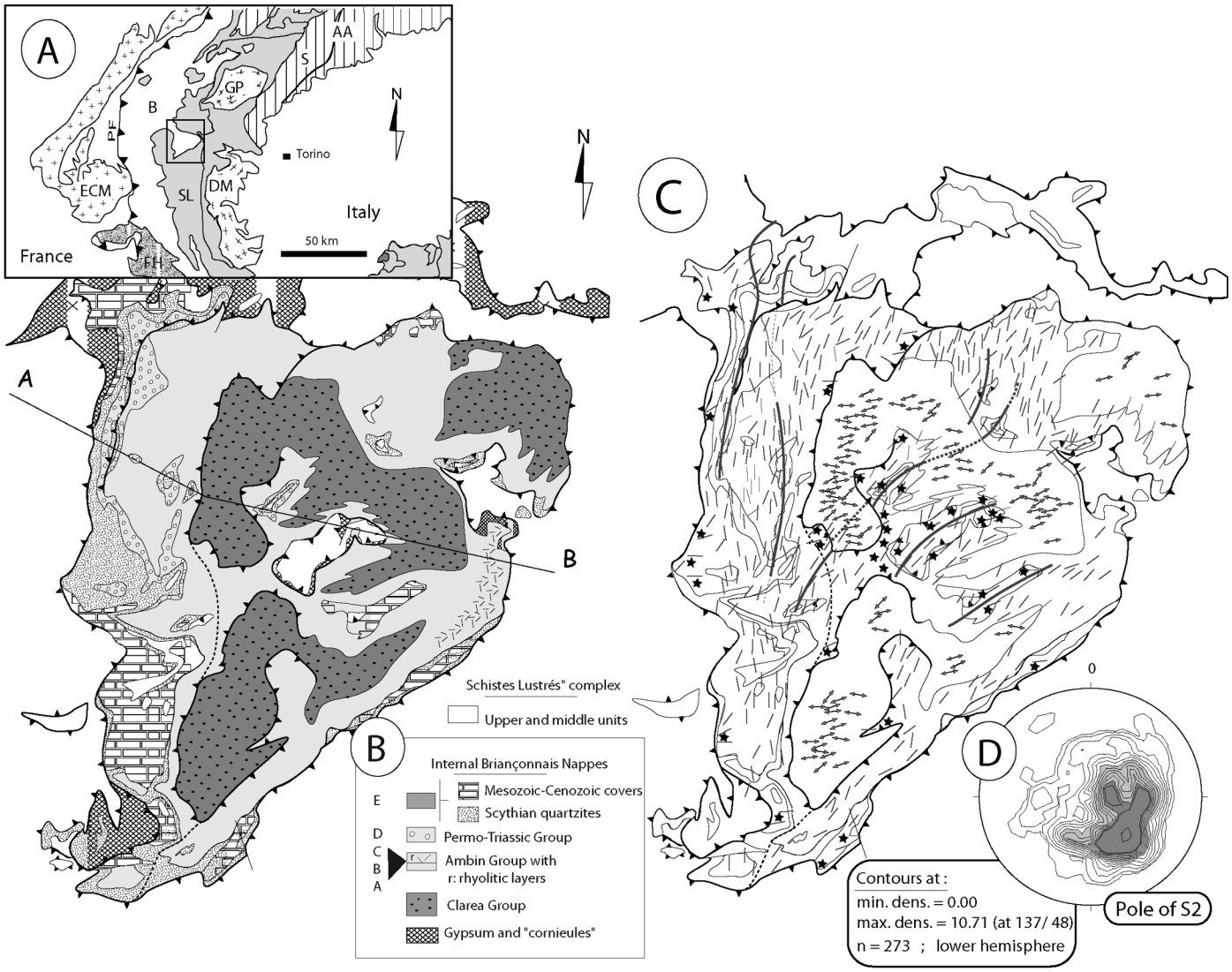

FIG.1 – Geological setting of the Ambin massif. (A) The study area within the northwestern Alps. ECM = External Crystalline massifs; B = Briançonnais domain; SL = "Schistes Lustrés" units where eclogitic and non-eclogitic units are separated by a line [after Pognante, 1991] ; GP and DM = Internal Crystalline massifs of Dora Maira and Gran Paradiso; FH = Helminthoid flysch nappes; AA = Austroalpine domain (S = Sesia); PF = Penninic front. (B) Geological sketch map of the Ambin massif based on mapping by Malavielle [1982], modified. The different *formations* (namely, A, B, C, D and E; see text) discussed in this paper have been reported on the lithological log previously established by Gay [1971]. Surrounding "Schistes Lustrés" units are unornamented. AB = trace of the geological cross-section (fig. 6). (C) Folds map. Double-arrows = F1 folds in the Claréa Group; dark small-lines = F2 folds in the Ambin Group; dark thick lines = F2 large-scale folds in the Ambin Group; dark stars = F2 sheath-folds located along the Φ2 tectonic-contacts (dark barbed wire). (D) Stereographic plots of poles to S2 foliation in the Ambin Group and overlying units (Etache Group, Briançonnais covers + Schistes Lustrés); northwestern side of the Ambin massif.

FIG. 1. – *Cadre géologique du massif d'Ambin.* (A) *Contexte général.* ECM = *Massifs cristallins externes ;* B = *domaine Briançonnais ;* SL = *nappe des Schistes Lustrés comprenant une partie éclogitique et une partie non-éclogitique [d'après Pognante, 1991] ;* GP *et* DM = *Massifs cristallins internes du Gran Paradiso et de Dora Maïra ;* FH = *nappes des Flyschs à Helminthoïdes ;* AA = *domaine Austro-Alpin (*S = *Sesia) ;* PF = *Front pennique.* (B) *Carte géologique du massif d'Ambin.* (C) *Carte des axes de plis.* (D) *Projections stéréographiques des pôles de foliation S2 échantillonnés dans la partie NW du massif.*

many discontinuous lenses (10 m to + 100 m thick), squeezed in between the overlying Schistes Lustrés and the basement (fig. 2C). They also form complex "klippen" on top of the Ambin dome that are refolded together with the Schistes Lustrés. The post-Permian stratigraphical sequence is highly variable: (1) in the Gran Scala area, discontinuous lenses comprise a thin quartzitic horizon overlain by Jurassic to Eocene marbles and schists; (2) at the Pointe de Bellecombe, a thicker sequence (> 200 m) includes the Scythian quartzites, Middle Triassic dolomites, Jurassic limestones and Cretaceous to Eocene phengite-rich marbles and schists; (3) southeast of the Ambin massif, several superimposed units have been recently distinguished [Polino *et al.,* 1999].

The ***Piemont*** and ***Liguria-Piemont*** terrains consist respectively of continental units from the European palaeomargin and oceanic units from the paleo-Piemont ocean [Deville, 1987; Fudral, 1998]. The continental units are mostly represented by the paragneiss and orthogneiss of the Gran Paradiso massif**,** with locally thin Mesozoic sedimentary covers (fig. 1A) and appear as tectonic windows, beneath the oceanic units of the Schistes Lustrés.

The ***Schistes Lustrés*** consist of remnants of oceanic crust (metagabbro and metabasalts) with overlying marine metasediments [for a synthesis see the work of Deville *et al.,* 1992]. Jurassic to Cretaceous in age, they represent an ocean-derived ophiolitic assemblage with associated pelagic to clastic sediments (calcschists). A major tectonic contact discontinuously outlined by gypsum or "cargneules", separates the "Schistes Lustrés" from the Ambin basement and from the Briançonnais lenses. The tectonic-lithological units previously defined in the "Schistes Lustrés" [Deville *et al*., 1992; Fudral *et al.,* 1987; Fudral, 1998] are resting obliquely against the contact with the basement. Except for the structurally lowermost eclogitic unit occurring near Susa, they are all correlated with the Combin Zone defined in Switzerland and Aosta valley [Caby *et al.,* 1996]. The Schistes Lustrés are divided into three subsets: a structurally lower unit, which contains a high percentage of metabasites (lower unit) and the structurally higher two units which contain a much lower proportion of metabasites (the median and upper units). This subdivision is based on lithology: the lower unit (LU) is mainly made up of serpentinites, metagabbros and metabasalts with some pelitic schists, whereas the median unit (MU) is mainly made up of carbonaceous pelites with some metabasalts. These two units, which are also characterized by their respective pressure peaks (D1 syn-metamorphic in the blue schists facies-MU, and in the eclogite facies-LU), were affected by a post-HP, ductile deformation, that culminated under greenschist facies conditions [Deville *et al.,* 1992; Rolland *et al.,* 2000; Agard, 2001 et 2002]. Such post-HP deformation correlates with the D2 phase previously defined in the Ambin and South Vanoise basements. In order to show this structural bond, we undertook a survey of the Piemont and Liguria-Piemont units that focused more precisely on the nature

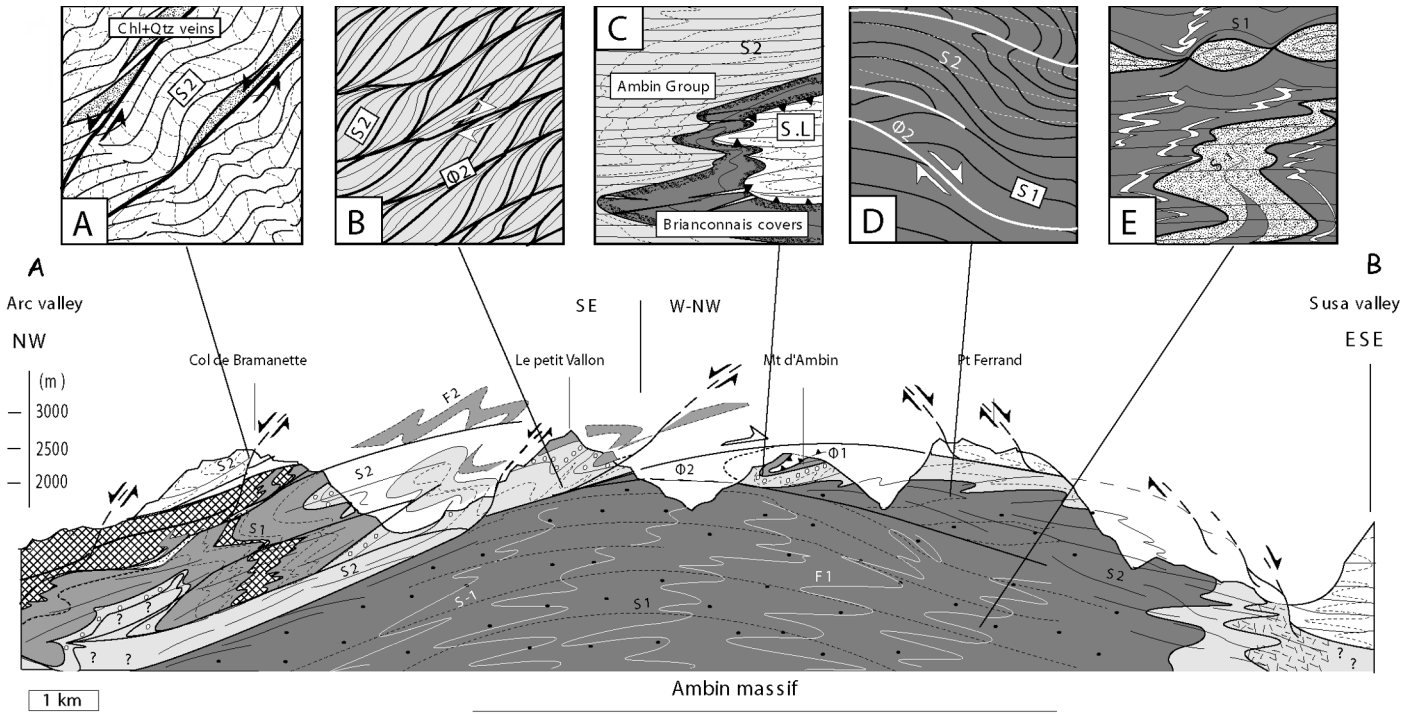

FIG. 2. – A synthetic cross-section of the Ambin massif (see fig. 1 for location). The dome defined by the D2 fabrics is enhanced by D3 brittle-ductile shear bands. (A) D3 shear band in the "Schistes Lustrés" units. (B) detail of the main Φ2 shear zones. (C) Refolding of the Φ1 structure. Dotted lines = S1 foliation; dark barbed wire = Φ1 tectonics contacts; S.L: "Schistes Lustrés" units). The inner part of the massif (i.e the Claréa Group) has been partly preserved from post-D1 deformations. (D) foliations pattern in the upper part of the Claréa Group. F1, F2 = Alpine folds. (E) Steeply-dipping quartz veins outlining the S-1 pre-Alpine foliation).

FIG. 2. – *Coupe géologique synthétique à travers la structure en dôme du massif d'Ambin.* (A) *Shear band D3 dans la nappe des Schistes Lustrés.* (B) *Détails sur une shear zone Φ2*. (C*) Détails sur les structures alpines précoces D1 au cœur du groupe micaschisteux de la Claréa.* (D) *Relations structurales entre fabrique S1 et S2 dans la partie supérieure du groupe de la Claréa.* (E) *Fabrique anté-alpine soulignée par des veines de quartz.*

and direction of the shearing under greenschist facies conditions.

STRUCTURAL EVOLUTION

A detailed structural geology map of the Ambin and South Vanoise massifs enabled us to highlight the large structural features of the Internal Briançonnais basements. In particular, the existence of three distinct events of intense Alpine ductile to brittle-ductile deformations (D1, D2 and D3) has been characterized at all scales by quite specific verging and foliations [Ganne *et al.,* 2003]. To summarise the structural evolution of the Ambin and South Vanoise massifs, structures and metamorphic assemblages related to D1 have been evidenced in all units now separated by large-scale Φ2 shear zones [Ganne *et al.,* 2005]. Concerning the D2 and D3 stages, the pattern is more complex and suggests a strong partitioning of the deformation. A dominant, non-coaxial extension, close to the shear zones (general eastward movement direction for Φ2, and conjugated eastward and westward movement for D3 small scale shear zones) grades to a coaxial component in between. In the Ambin massif, deformation more particularly characterizes two different settings: (1) the core of the tectonic pile, made up exclusively of the Claréa Group (metapelites), preserve an early Alpine deformation (D1). This deformation displays a HP-LT mineral assemblage (garnet-jadeite-glaucophane-clinozoisite-chloritoid) with a strongly penetrative, north-directed shear fabric (fig. 3 and fig. 4). (2) The various envelopes of the Ambin Group, Briançonnais cover and Schistes Lustrés are intensely affected by D2, an east-directed shear deformation, which was continuous and syn-metamorph from the time of crystallisation of glaucophane to the greenschist facies stage (fig. 5). The upper parts of the basement domes are mostly affected by this D2 deformation (fig. 6), with the major part of the core preserving the earlier D1 Alpine structures. The end of the second Alpine event, which we have named D3, is characterized by structures that were formed in much colder conditions, and that accompany the late doming of the Ambin massif.

The early tectono-metamorphic evolution of the lowest metapelitic sequence (i.e. the Claréa Group) has previously been described by Ganne *et al.* [2005]. The purpose of this paper is not to re-investigate the D1 event but to give an overview of how strain, structures and mineral phase assemblages linked to the subsequent D2 ductile and brittle-ductile D3 events are distributed throughout the surrounding Ambin Group and overlying oceanic units of Schistes Lustrés.

Ductile structures in the Ambin Group

The structure of the Ambin Group is dominated by a pervasive, post-HP, subhorizontal foliation (S2) developed in the glaucophane-chlorite facies [Ganne *et al.*, 2005], a P–T

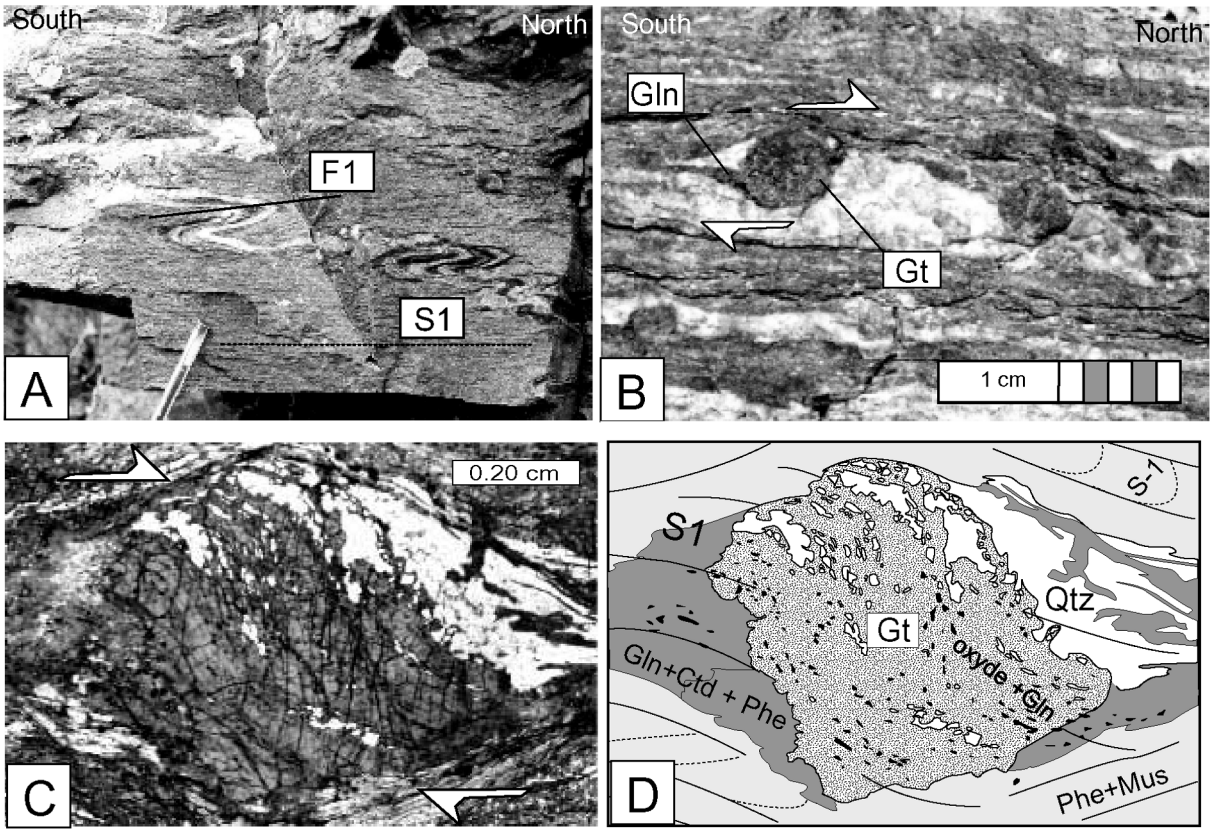

FIG. 3. – D1 deformation patterns in the Claréa Group. (A) pre-Alpine mineral foliation of biotite (dark bands) - muscovite-quartz refolfded by Alpine F1 fold; Alpine HP mineral assemblage grows in the S1 axial foliation. (B, C and D) Alpine syn-kinematic garnet (Gt; Ga-35) surrounded by HP minerals forming a strain fringe of glaucophane (Gln) ± chloritoid (Cld) ± phengite (Phe). Note the trails of oxides and glaucophane inclusions in the garnet (fig. 4D), outlining the S1 foliation.

FIG. 3. – *Caractéristiques minéralogiques des micro-structures D1 au cœur du groupe de la Claréa.* (A) *Assemblages métamorphiques anté-alpins.* (B, C and D) *Grenats alpins syntectoniques.*

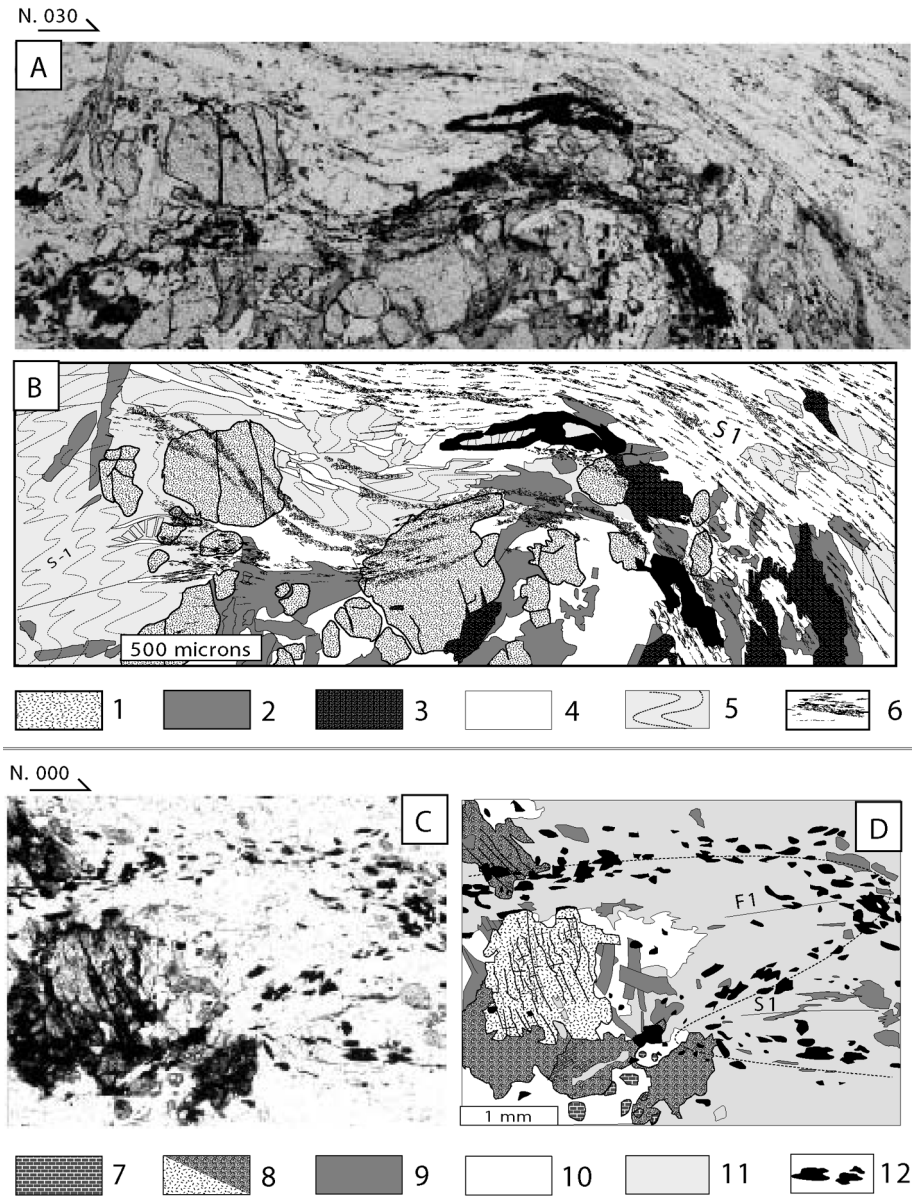

FIG. 4. – D1 high-pressure minerals in GBM. (A and B) garnet-glaucophane-chloritoid-phengite assemblage defining the S1 foliation (sample Ga-53). [1] = garnet (Gt); [2] = chloritoid; [3] = glaucophane; [4] = mixed Alpine HP-minerals in possible pseudomorphs of staurolite; [5] = inherited muscovite underlyning a pre-Alpine foliation (S-1); [6] = High-Si substituted phengite outlining the main Alpine foliation (S1). (C and D) jadeite-glaucophane-garnet assemblage (sample Ga-51) overprinting the hinge of a F1 Alpine fold. F1 is marked by trails of opaque minerals. [7] = small type-3 garnet; [8] = jadeite ; [9] = glaucophane; [10] = quartz; [11] = mixed of high-Si substituted Alpine phengite and pre-Alpine muscovite; [12] = opaque minerals
FIG. 4 – *Minéraux D1 de haute pression dans les micaschistes à glaucophane du groupe de la Claréa* (GBM). (A *et* B) *Micaschistes à glaucophane.* (C *et* D) *Micaschistes à jadéite.*

domain equivalent to the greenschist-blueschist metamorphic transition of Evans [1990]. This main-phase foliation is parallel to the contact of the Ambin Group with the overlying oceanic units of Schistes Lustrés and defines the broad regional dome structure. An E–W-trending stretching lineation (L2) is associated with this flat-lying foliation [Gay, 1971]. Several authors proposed that this main fabric was generated in a context of continental collision (shortening structures) and associated with top-to-the-west sense of thrusting [Malavieille, 1982; Allenbach, 1982]. Based on (i) new structural and petro-microstructural mapping, (ii) systematic measurements of fold axes, foliation and stretching lineations, (iii) recognition of shear criteria, and (iv) identification of strain gradients, from map-scale Φ2 mylonitic zones of Alpine age to low-strain domains preserving early D1 HP-structures in the core of the Claréa Group, Ganne *et al.* [2003, 2005, 2006] re-interpreted this main D2 deformation as linked to a major extensional event (detachment) with top-to-the-east sense of shearing.

Planar fabrics and meso- to macro-scale folds

The banded micaschists and metagreywackes of the Ambin Group as well as the overlying oceanic units of Schistes Lustrés share a common post-HP foliation (S2) indicating that the regional fabric in these rocks formed contemporaneously. Microscopic analysis suggests that the main ductile deformation (D2) occurred under retrograde metamorphic

conditions, because the S2 foliation spans a large range of mineral association, from the growth of glaucophane in equilibria with high-substituted phengites to the large development of middle-substituted phengite-chlorite-albite ± paragonite ± brown to green biotite.

Stereographic plots of foliation poles in the micaschists and banded metagreywackes of the Ambin Group, and in the overlying oceanic units of calcschist with intercalated mafic bodies of dm-scale are shown in figure 1d. This stereographic plot concerns the northwestern part of the Ambin massif that we studied in more detail to draw up its lithological evolution. In spite of the obvious influence of later folding by D3 doming (see below), the clear dominance in both cases of gentle- to moderately-dipping foliations reflects a previous sub-horizontal fabric. The similarity in foliation orientation and in metamorphic grade suggest that the S2 foliation in these two groups of rocks formed during the same tectonic event. Only differs the peak of D1 metamorphism that is rather different in age and pressure-temperature conditions [see Ganne *et al.,* 2006 for discussion].

The main S2 foliation was subsequently affected by outcrop– to map-scale folding. These NS-trending folds are characterized by different vergence or structural expression, namely with: (i) weakly west recumbent to inclined folds of the *Pointe de Bellecombe* cliff, (ii) E-verging upright open to gentle folds in the eastern side of the massif and (iii) W-verging upright gentle folds in the western side of the massif that in some case cause inflexions of the axial traces of earlier D2 formed folds. The occurrence of D2 intrafolial and synfoliation folds inside the main S2 foliation attests the existence of previous (F2) fold-forming events. Considering that, the above-mentioned folds will be referred to as F3.

Lineations and kinematics

Lineations (L2) in the micaschist of the Ambin Group are commonly defined by alignment of elongated crystals of glaucophane, chloritoid, fibrous phengite or biotite and stretched patches of chlorite. L2 lineations in the banded metagreywackes of the Ambin Group are mostly materialised by the dimensional shape-preferred orientation of quartz and ± albite poekiloblastic grains. The deformation fabric in few parts of the Ambin Group can be dominantly planar, so that stretching lineations are less common than in the other structural level having experienced high-strain of D2 shearing (Φ2 contact). The high strain coeval with lineation development is indicated by local occurrence of sheath folds [Quinquis *et al.,* 1978] in metapelites, of oblique folds [Passchier, 1986; also called asymmetric type folds, Holdsworth, 1990] in banded metagreywackes, and by common mylonitic fabrics close to the Ambin-Claréa Group tectonic contact on the northwestern side of the massif (the Lac Noir Φ2 shear zone).

At the outcrop scale, the orientation of lineations is very consistent, deviating by less than a few degrees, unless disturbed by later folds. Map-scale distribution shows gently plunging W- to WNW-trending lineations in the western part of the massif and E to ESE-plunging in the eastern part. Much of the dispersion observed at the scale of the map can be explained by reorientation caused by later folding and/or wrench shearing. In particular, inspection of figure 2b in Ganne *et al.* [2005] shows that most SE-trending lineations in metasedimentary rocks occur close to late D3 large-scale folding (outcropping in the *Pointe de Bellecombe* cliff). However, in most outcrops the banded metagreywackes and metapelite shows E-trending lineations, which may reflect an original orientation.

In the Ambin Group, a number of mesoscopic kinematic indicators in sections normal to the S2 foliation and parallel to the lineation point to non-coaxial deformation with top-to-the-east sense of shear. The most common are shear bands, s-type porphyroblasts of Na-feldspar (albite), asymmetrical boudins of quartz or quartz/albite aggregates, and rotated and transposed veins of chlorite-quartz. Mylonitic fabrics and shear criteria are easily seen at microscopic scale. This suggests that temperatures remained moderately elevated ($T < 500^oC$) for a long time, blocking grain growth to preserve syn-shear microscopic fabrics. Unequivocal shear sense criteria were observed in the calcareous sheets intercalated within the banded metagreywackes (formation B and C). In deformed rich-chlorite-epidote schists mapped in the eastern part of the massif (*Barrage St Nicolas*), asymmetric mafic enclaves and fold asymmetry locally suggest top-to-the-east shear sense.

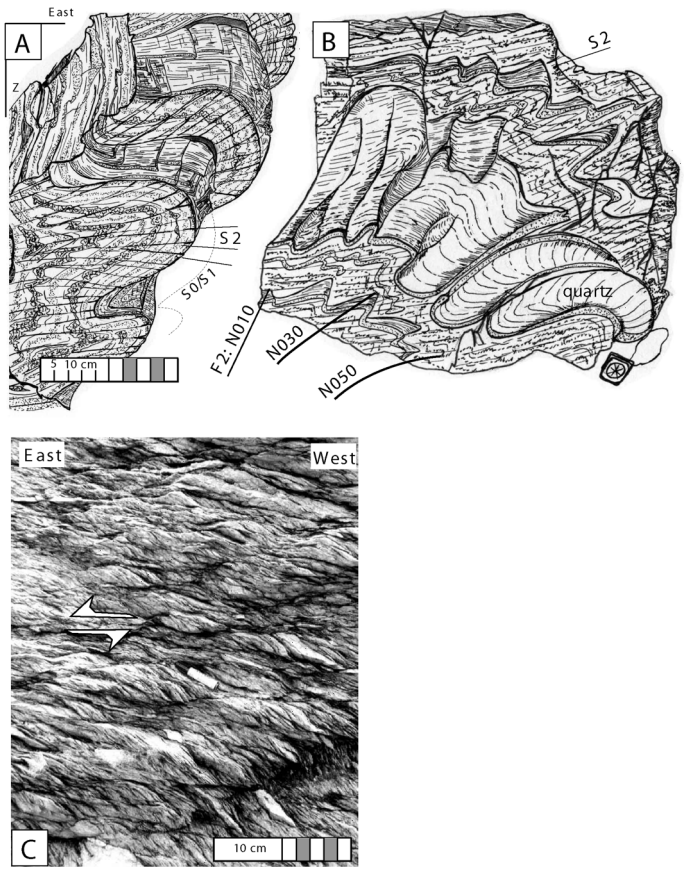

FIG. 5. – D2 ductile deformation in the Ambin Group. (A) Dominant N-S trending B-type fold. (B) NE-SW to E-W trending sheath-folds close to the Φ2 contacts ; (C) Pervasive ductile shear zone with top-to-the-east movement direction close the Claréa-Ambin Φ2 tectonic-contact.
FIG. 5. – *Caractéristique structurale et cinématique de la déformation ductile D2 dans le groupe siliceux d'Ambin.* (A) *Plis de type B à vergence Est.* (B) *Plis en fourreau à vergence Est à SE développés à proximité des contacts cisaillants Φ2* (C).

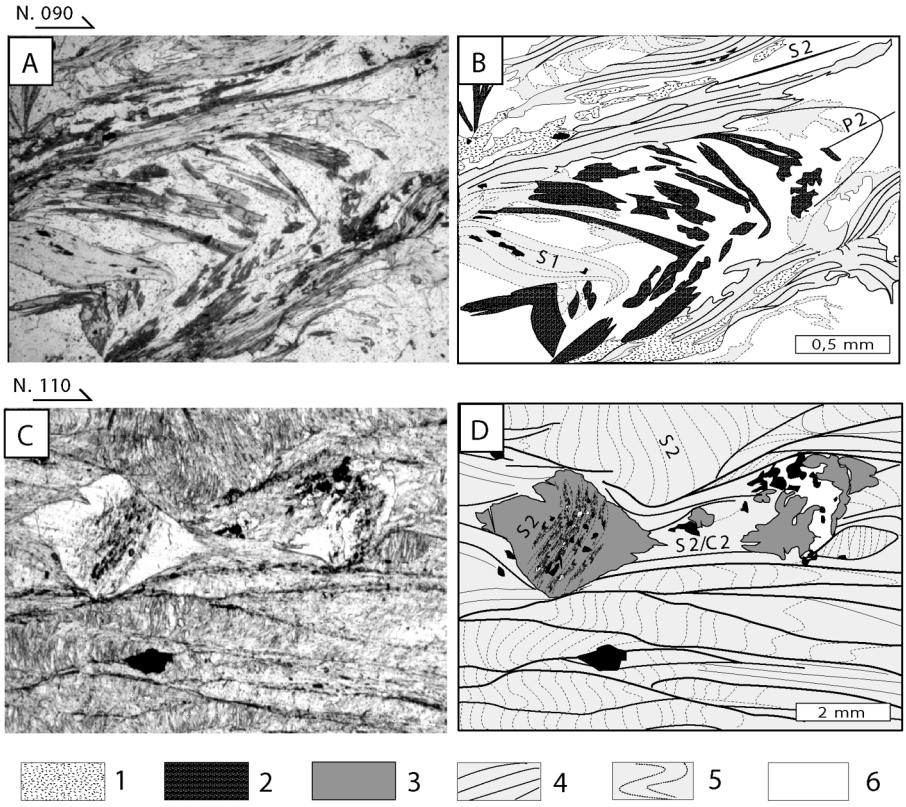

FIG. 6. – D2 microstructures in GBM. (A and B) D2 crenulations : reworked glaucophane and phengite in the S2 foliation. (C and D) D2 albite porphyroblast overprinting the S2 foliation; the sample occurs in a pervasive D2 shear zone (fig. 2B) where S2 and C2 plans are often parallel. (1) = chlorite; (2) = glaucophane; (3) = albite; (4) = D2 low-Si substituted phengite; (5) = D1 high-Si substituted phengite; (6) = quartz.
FIG. 6. – *Microstructure D2 dans les micaschistes à glaucophane du groupe de la Claréa* (GBM). (A *et* B) *Crénulation* D2. (C *et* D) *Porphyroblastes d'albite de génération D2.*

Strain partitioning of the shear deformation in the Ambin Group

Φ2 high-strain zones in the Ambin Group are hosted in part by variably calcareous quartzo-feldspathic wackes and subordinate metapelites (formation A, B and C, see above). Effects of ductile shearing and phase mineral equilibria in these rocks vary considerably, depending on strain intensity and geographic location within the Ambin Group. For example, albite development appears to have increased with depth along a vertical strike. This may be due to increased crust depth with elevated temperature but perhaps also to some extent to elevated fluid flow accompanying shear zones development (work in progress). Strain partitioning of the high-shear deformation, in the environment of high-pressure / low temperature (HP-LT), can be discussed at the scale of the *Lac Noir* and *Lac d'Ambin* areas outlining the lowest parts of the Ambin Group. There, rocks are exclusively represented by the A and B-type formation (see above). Ductile strain was concentrated in metagreywacke-metapelitic horizons, controlled largely by the behaviour of the phyllosilicates.

Medium-strain portions of the *Lac Noir* and *Lac d'Ambin* areas are identical to that commonly observed in the whole tectonic pile of the Ambin Group, except an interlayered highest strain portion that is a continuously mappable zone of albite-rich mylonite (Φ2 tectonic contact). Gradational relationships between this medial zone of dm-scale and the flanking phengite-chlorite-rich lower strain rocks suggest that strain heating, concentration of mineralised fluids in the high-strain zone, or a combination of the two mechanisms was responsible for generation of the albite (work in progress).

Metapelites and metagreywackes

Fine-grained metapelites (phyllonite *s.s.*) and coarser-grained metagreywackes dominate the medium strain zones in the *Lac Noir* and *Lac d'Ambin* areas. Primary sedimentary features are mostly obliterated in metapelitic zones rather than in the metagreywackes rich-zones by penetrative shear-generated foliation (S2/C2) caused by the D2 ductile deformation. Metapelitic S2/C2 fabric is defined by phengite-chlorite ± glaucophane ± chloritoid elongated flakes and some stretched biotite, and typically anastomoses in areas of highest shear strain. Detrital mm- to cm-scale quartz grains in quartzo-feldspathic wackes interlayered with the metapelite are plastically deformed and flattened or elongated to develop grain-shape-preferred fabrics. Sub-grain rotation recrystallization of quartz is only common in areas of the highest strain. Grain-size reduction due to dynamic recrystallization and sub-grain development is common, producing a very fine-grained texture typically around 0.3 μm or less. Microscopic S2/C2 or S2/C'2 structures are developed in interlayered cm-scale metapelites.

Mylonite

The highest-strain part of the *Lac Noir* and *Lac d'Ambin* areas is a belt of schistose mylonite that differs from the metapelites and metagreywackes in that it is more schistose and sheared (remarkable *fish structures,* fig. 5C) and has more recrystallized albite grains than are found anywhere else in the Ambin Group. This high-strain zone is approximately 50 m wide and passes gradationally into typical fine-grained metapelites and metagreywackes. The zone of schistose mylonite contains voluminous pale gray to white and fine-grained quartz veins, < 1 mm to 5 cm thick. These are evenly distributed throughout the schistose mylonite zone but are sheared and boudinaged, implying significant fluid involvement before and/or during ductile shearing. The flux of silica-rich fluids silicified the pre-existing metasedimentary rocks. Quartz veins and detrital quartz and feldspar grains in wacke were completely recrystallized, and coarse to very coarse albite define, together with phengite, chlorite and biotite flakes, a penetrative S2/C2 fabric. Recrystallization may have been caused by elevated heat flow from deeper crustal levels toward the end of ductile shearing, presumably related to fluid migration in the high-strain zone.

Brittle-ductile structures in the Ambin Group

A late brittle deformation (D3) is displayed by several NS-trending, high-angle, normal Φ2 brittle-ductile faults that moderately affect the entire Ambin Group tectonic pile, cutting across lithological as well as tectonic boundaries. D3 deformation features include large-scale open folds affecting the previous S2 foliation and a locally developed S3 micaceous crenulation. D3 is commonly marked in the overlying oceanic units of Schistes Lustrés by small-scale NS-trending crenulation-folds overprinting the D2 structures. In some instances, their walls contain low-substituted phengite, chlorite, quartz and calcite crystals. Brittle-ductile shearing, generated along the Φ3 plans, penetrated only a few meters into adjacent rocks. There, the dominant deformation mechanism was pressure solution mass transfer that produced a very penetrative close-spaced anastomosing S3 cleavage (the main fabric at the outcrop scale). The Φ3 faults display a large range (from a few cm to several dm) of offset. They are thus not of negligible importance for the large-scale domal structure of the studied area [Ganne *et al.,* 2005]. Similar brittle, late-metamorphic faults have been described further northeast of the studied area, in the Vanoise and Gran Paradiso National Parks [Rolland *et al.,* 2000; Le Bayon and Ballèvre, 2006].

Ductile to brittle structures in the Piemont and Liguria-Piemont units

In the Gran Paradiso and in the Schistes Lustrés, the shear zone patterns are slightly different. East-directed, ductile shearing that operated mainly in the lawsonite-greenschist facies metamorphism affected the Median oceanic units located at the edge of the Ambin and South Vanoise massifs. As we have shown for the basement units [Ganne *et al*.,

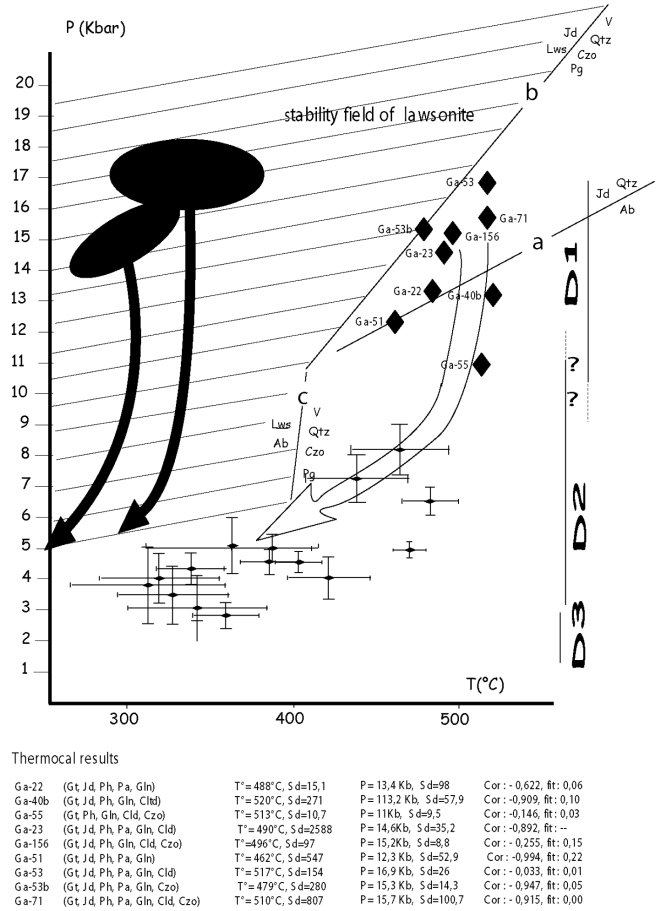

FIG. 7. – Calculated P-T path for the GBM. For the Thermocalc results [Holland and Powell, 1998], each symbol corresponds to a specific D1 mineral assemblage (dark diamond); The error on each calculation is proportional to the value of the "fit" [Holland and Powell, 1998]. Fit = sigma(fit) = the scatter of the residuals of the enthalpies and the activities normalised by their uncertainties. Corr = correlation coefficient between calculated P and T. For the Tweeq program [Berman, 1991], each symbol corresponds to a specific D2 mineral assemblage (error bars). Reaction curves : (a) albite (Ab) = jadeite (Jd) + Qtz [Holland, 1980], (b) lawsonite (Lws) + Jd = zoesite (Zo) + paragonite (Pg) + Qtz + H_2O and (c) Lws + Ab = Zo + Pg + Qtz + H2O [Heinrich and Althaus, 1988]. Thermodynamic data and corresponding solid solutions for Tweeq calculations are indicated in the text. Dark arrow: P.T path for the surrounding "Schistes Lustrés" units from Agard *et al.* [2001].

FIG. 7. – *Chemin P-T calculé pour le socle du massif d'Ambin. Les losanges noirs correspondent aux estimations P-T réalisées avec le logiciel Thermocalc sur des assemblages D1 provenant de 10 échantillons du type Groupe de la Claréa. Ces estimations sont fournies en bas de la figure. Les croix noires correspondent aux estimations P-T réalisées avec le logiciel Tweeq sur des assemblages D2 provenant de cinq échantillons du type Groupe d'Ambin. La taille des croix est proportionnelle aux marges d'erreur. Courbes de réaction :* (a) *albite (Ab) = jadéite (Jd) + Qtz [Holland, 1980],* (b) *lawsonite (Lws) + Jd = zoïsite (Zo) + paragonite (Pg) + Qtz + H2O and* (c) *Lws + Ab = Czo + Pg + Qtz + H_2O [Heinrich and Althaus, 1988].*

2005], penetrative shearing develops concomitantly with the main foliation of the rock. The main foliation plane corresponds to a composite surface (S2) that resulted from the tectonic transposition of lithological surfaces (S0) and early tectonic structures (S1) during D2 shearing. Metamorphic minerals occurring on the S2/C2 shear planes generally correspond to HP mineral assemblages (fig. 10A) retrogressed under greenschist facies conditions. The stretching lineation associated with such planes presents a remarkably constant orientation (~N100), which is either parallel to sheath-fold axes (N090) or to D1-D2 interference folds (N075 with N110) which are associated with the major Φ2 tectonic contacts. In between major shear zones, the orientation of the F2 fold axes is N-S with an apparent verging preferentially towards the east (fig. 11B). The isoclinal, F2 folds, of centimetre to decametre scale, are often truncated by late shearing of the Φ2 shear zones. A later and much colder deformation (D3) superimposed a doming structure onto the Φ2 structures. S3 fracture crenulations and very steeply-dipping shear planes (F3) developed respectively with east and west verging on both sides of the massif. Geometrically, the opposing dip-direction of the major Φ2 contacts between the Briançonnais basement and the median units of the Schistes Lustrés is due to this late doming.

To the west of the Gran Paradiso, a major D2 tectonic contact separates the median and lower units of the Schistes Lustrés. Having been identified in the literature for many years, this west-dipping contact has been traced out by the presence of either serpentinite or cargneule lithologies. Many authors describe this contact as a ductile normal fault partly responsible for the exhumation of HP-LT units [e.g. Ballèvre *et al.,* 1990 or Rolland *et al.,* 2000]. Other authors have interpreted it as an east-directed backthrust responsible for the juxtaposition of oceanic units atop the Gran Paradiso basement [Chopin, 1981; Deville, 1987]. We followed this major contact (of N-S orientation) from *Bonneval* to the *Susa valley* (fig. 9). The direction of movement (marked by stretching of chlorite) observed within the S2/C2 shear bands indicates a displacement towards the west. The associated F2 folds also present an apparent verging towards the west. This dominantly west-directed shear regime, of apparent normal movement, is also observed at the contact between Gran Paradiso and lower unit of the Schistes Lustrés (fig. 10C), and even within the median unit along the so-called "*digitation de l'Iseran*" [Deville, 1987] (fig. 9). The major Φ2 contacts locally appear deformed by D3 (undulations of the S2/C2 planes with the development of a S3 cleavage fracture; fig. 11A).

In between the Briançonnais basement domes of Ambin (South Vanoise) and Piemont (Gran Paradiso), a dominant D2, flat-lying fabric is conspicuous within all the HP units. Conjugated shearing with eastward and westward movement direction led to a boudinage of the S2 fabric and the development of F2 drag folds with opposite asymmetry (fig. 11C). This pattern indicates an overall "pure-shear" regime. This is generally observed in the areas away from the major Φ2 contacts, which are quite localised at the edge of the basement domes (see the Schistes Lustrés located between *Lanslebourg* and *Punta Ciamarella*, fig. 9). When these shear fabrics with opposite verging are present in the immediate vicinity of the major Φ2 contacts (fig. 9), strongly developed "fish structures" can be observed. In accordance with results of Celmas [1982] and Philippot [1988], who have shown that the sense of shearing can radically change across a zone of high-strain, we can consider that on the scale of our structures, opposite verging represent local kinematic heterogeneities associated with an overall shear regime of a single direction. This kilometric-scale, high-strain network of ± anastomosing, west-directed shear zones, stretches from the *Col de l'Iseran* (median unit) until the *Refuge des Evettes* (at the western edge of the Gran Paradiso massif).

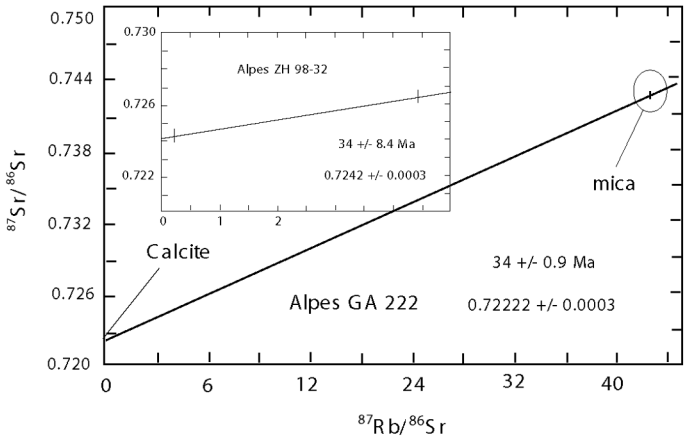

N° Sample	Rb tot (ppm)	Sr tot (ppm)	$^{87}Rb/^{86}Rb$	$^{87}Sr/^{86}Sr$ (2 σ)
ZH98-32 M	116.60	76.05	4.4463	0.726365(38)
ZH98-32 C	34.52	406.8	0.2460	0.724323(37)
GA 222 M	370.80	25.11	42.8540	0.742316(32)
GA 222 C	2.60	5401	0.0014	0.722235(26)

FIG. 8. – Rb/Sr diagram on the phengite/calcite pairs.
FIG. 8. – *Diagramme Rb/Sr sur le couple phengite/calcite.*

METAMORPHIC EVOLUTION

The data presented here concern mostly the Ambin massif. The reader will find mineral data for the Schistes Lustrés and Gran Paradiso in recent papers [see Goffé *et al.,* 2004 for review]. About 200 samples of garnet-bearing micaschists have been sampled in the Ambin massif (and in South Vanoise for comparisons). 15 thin-sections have been selected for microprobe analyses. Samples were analysed on a CAMEBAX SX-50 microprobe, at the University of Lausanne. Counting times were 15 to 30 s per element on peak and 5 to 30 s on background depending on concentrations. The accelerating voltage was 15 KV and the beam current 10 to 20 nA. Natural silicates were used as standards. Only a few selected analyses are given in this paper for reference (table I). The whole database appear in a brother paper devoted to garnet assemblages [Ganne *et al*., 2003]. The repartition of minerals according to the deformation stages is sketched on table I in Ganne *et al.* [2003].

Two populations of garnet may be distinguished [Ganne *et al*., 2003] in the Ambin massif from their grain size: large garnets (type-1 and type-2) and small garnets (type-3). Alpine garnets correspond to a solid solution of almandine (Xalm = 0.75-0.62), grossular (Xgros = 0.19-0.25), spessartine (Xspes = 0.0-0.16) and pyrope (Xpy = 0.01-0.08).

According to microstructural evidence, the zoning pattern and the inclusions distribution within garnets indicate that type-2 and type-3 garnets, as well as the rim of the large type-1 garnet grew during a HP Alpine stage. Only the core of type-1 large garnets is probably inherited from pre-alpine metamorphism. The Mn ⇔ Fe, ± Ca exchange in Alpine garnet is responsible for a growth zoning related to a gradual increase of P.T conditions (depletion of Mn toward the edge of crystals). A good correlation was observed between, on one hand, the distribution of phengite inclusions in garnet and their tschermakitic substitution and, on the other hand, the distribution of blue amphibole inclusions in garnet and their Al (IV) content. The most Si-substituted phengites and Fe-glaucophane are located close to the edge of the crystals [Ganne *et al.*, 2003].

Glaucophane and phengite inclusions are thus related to prograde HP metamorphism of Alpine age. Conversely, the scattering of garnet compositions along the Fe, Mg ⇔ Ca axis, with alternating Fe or Ca depletion toward the edge of crystals, is more ambiguous. It may correspond either to the last growth stage of Alpine garnets during the prograde evolution or to the retrograde P-T path.

Chloritoid occurs as individual crystals in the S1 foliation and was never observed as inclusions in garnet. It shows a X_{Mg} value varying between 0.07 and 0.14 and no significant pattern from core to rim.

Blue amphibole related to the S1 foliation plots in the ferro-glaucophane field of the IMA classification [Leake, 1978]. Variation of the X_{Mg} value is restricted to an occasional slight decrease of the magnesium content from core to rim. Glaucophane inclusions occurring in garnet show a lower MgO content (in the range 1.8 to 5.68 mol %) and a higher manganese content (in the range 0.12 to 0.23 mol %) than the large glaucophane crystals developed in the groundmass.

In biotite-schists Na-clinopyroxene occurs as tiny inclusions within albite (X_{Jd}: 0.88). It is less abundant in blueschists (X_{Jd}: 0.55). In both rock types inclusions of jadeite in garnet was not observed.

Chlorite shows X_{Mg} values ranging from 0.3 and 0.5.

The maximum celadonite content of phengite ranges from Si^{4+} = 3.53 to 3.60 and XMg values vary from 0.53 to 0.75. No significant difference of the maximum Si content is observed between blueschists and biotite-schists. A core-to-rim decrease of the Si content is observed in most samples varying from sample to sample. The most substituted phengites were found as inclusions in the external rim of Alpine garnets. Their Si^{4+} content ranges from 3.35 to 3.60. Syn-kinematic phengites, with $3.10 < Si^{4+} < 3.55$, which define the two Alpine foliations (S1 and S2) are sometimes interlayered with paragonite. The colourless patches of phengite, associated with the D3 shear zones, are characterised by very low- Si^{4+} contents (< 3.08).

Clinozoisite does not show significant compositional zoning. This mineral shows $Fe^{3+}/(Al+Fe^{3+})$ ratios ranging from 0.25 to 0.27. Albite is close to the end-member

TABLE. I. – Selection of microprobe analyses and structural formulae used for Thermocalc (D1 assemblage) and Tweeq (D2 assemblage) multi-equilibrium calculations. Incl = inclusion; mt = matrix. Note that glaucophane inclusions in garnet show lower magnesium content and a higher manganese content when compared to matrix glaucophane. Samples were analysed on a CAMEBAX SX-50 microprobe, at the University of Lausanne. Counting times were 15 to 30 s per element on peak and 5 to 30 s on background depending on concentrations. The accelerating voltage was 15 KV and the beam current 10 to 20 nA. Natural silicates were used as standards.

TABL. I. – *Sélection d'analyses microsondes sur les micaschistes du socle d'Ambin, utilisées pour les calculs en multi-équilibres (Thermocalc et Tweeq).*

	Garnet						Glaucophane		Jadeite		phengite		Chloritoid	Clinozoisite
Label	40b-1/33	40b-1/12	40b-1/1	70-2_37	70-2_1	53_37	23-2/Gln	71-13/Gln	23-23/Jd	71-23/Jd	23-6/mu	71-52/mu	23-3/Cld	71-9/Czo
Rock		ABM		ABM		GBM	ABM	GBM	ABM	GBM	ABM	GBM	ABM	GBM
Type		type 1		type 2		type 3	mt	incl	mt	mt	incl	incl	mt	mt
	core	rim 1	rim 2	rim	core									
SiO2	35.37	35.25	36.47	36.04	36.03	37.65	56.03	55.2	57.9	57.86	51.83	54.24	23.6	37.96
TiO2	0.38	0.06	0.07	0.10	0.16	0.10	0.1	0.16	0.03	0.03	0.37	0.14	0.06	0.06
Al2O3	20.25	20.53	20.82	20.68	20.31	20.72	11.16	10.74	17.28	15.77	25.1	27.09	39.37	23.09
Cr2O3							0.07	0.05	0.01	0	0.02	0.02	0.02	0.05
Fe2O3							0	0.47	5.8	9.24	0	1.86	1.88	12.5
FeO	25.85	30.96	29.70	33.62	28.45	33.19	14.69	16.19	3.68	2.79	3.39	1.67	24.09	0.11
MnO	10.19	5.31	2.58	0.30	5.31	0.89	0.02	0.18	0	0.05	0	0.05	0.47	0.19
MgO	1.17	2.13	1.82	2.00	0.96	1.29	6.96	5.61	0.17	0.31	3.5	2.79	1.93	0.14
CaO	5.46	4.27	7.46	6.87	7.92	6.39	0.53	0.2	0.54	0.45	0.03	0.01	0.05	20.42
Na2O							6.6	7.47	13.92	14.07	0.07	0.11	0.01	0.07
K2O							0.02	0.01	0.01	0	10.71	6.73	0.05	0.79
total	98.67	98.51	98.91	99.60	99.14	100.23								
Totals							96.18	96.28	99.34	100.58	95.03	94.71	91.54	95.38
Oxygens	12	12	12	12	12	12	23	23	6	6	11	11	6	12.5
Si	2.93	2.92	2.96	2.93	2.95	3.02	7.97	7.948	2.039	2.03	3.485	3.536	0.993	3.083
Ti	0.02	0.00	0.00	0.01	0.01	0.01	0.011	0.017	0.001	0.001	0.019	0.007	0.002	0.004
Al	1.98	2.00	1.99	1.98	1.96	1.96	1.872	1.823	0.717	0.652	1.989	2.082	1.953	2.211
Fe	1.79	2.14	2.02	2.29	1.95	2.23								
Cr							0.008	0.006	0	0	0.001	0.001	0.001	0.003
Fe3							0	0.051	0.154	0.244	0	0.091	0.06	0.764
Fe2							1.748	1.949	0.108	0.082	0.191	0.091	0.848	0.008
Mn	0.71	0.37	0.18	0.02	0.37	0.06	0.002	0.022	0	0.001	0	0.003	0.017	0.013
Mg	0.14	0.26	0.22	0.24	0.12	0.16	1.476	1.204	0.009	0.016	0.351	0.271	0.121	0.017
Ca	0.48	0.38	0.65	0.60	0.70	0.55	0.081	0.031	0.02	0.017	0.002	0.001	0.002	1.777
Na							1.82	2.086	0.951	0.958	0.009	0.014	0.001	0.011
K							0.004	0.002	0	0	0.92	0.56	0.003	0.082
TOTAL	8.06	8.08	8.03	8.07	8.06	7.99								
Mn/Fe							0.001	0.011	XMg 0.08	0.16	XMg 0.65	0.75	0.12	$\frac{Fe(3+)}{Fe(3+)+Al}$ 0.25
									X Jd 0.71	0.65				
XMg	0.07	0.11	0.10	0.10	0.06	0.06								
Alm	57.13	67.88	65.84	72.65	62.27	74.50								
Sps	22.81	11.78	5.79	0.65	11.77	2.02								
Py	4.61	8.34	7.19	7.69	3.76	18.31								
Grs	15.45	12.00	21.18	19.02	22.21	18.31								

composition, with a maximum anorthite content of 0.01 mole per cent. Biotite and stilpnomelane are occasionally present as retrograde phases. Discrimination between oxychlorite, chloritised biotite and inter-grown stilpnomelane and chlorite was not possible from the available microprobe analyses. Rutile is nearly pure.

P-T estimates

The equilibrium P-T conditions corresponding to D1 assemblages (Grt-Cld-Gln-Czo-Jd-Rt) have been calculated with the Thermocalc software [Holland and Powell, 1998]. For the high-variance D2 mineral assemblages involving Chl, Phg, Ab, Pg and Qtz, no P-T estimates have been obtained with Thermocalc. We therefore used the multi-equilibrium approach proposed by Vidal and Parra [2000] along with the thermodynamic data and solution models of Vidal *et al.* [2001] for chlorite and Parra *et al.* [2002a] for phengite. This method has been successfully used by Trotet *et al.,* [2001a and b]; Bosse *et al.,* [2002] and Parra *et al*. [2002b] for similar rocks. Calculations were performed with the Tweeq and Intersx softwares [Berman, 1991], assuming a water activity equal to unity. The error bars on figure 7 are proportional to the scattering of the intersection points among all the equilibria that can be calculated from the five-components solid solution model for chlorite and from the six-component model for K-white mica [see Berman, 1991; Vidal and Parra, 2000 for details]. The uncertainty on the P-T estimates is probably less than 1 kbar, 30°C [Vidal and Parra, 2000; Trotet *et al*., 2001a].

New Tweeq calculations are currently in progress on HP assemblages in order to fill the gap on the diagram (fig. 7) between Tweeq and Thermocalc P-T estimates. For that purpose we added new data in the Tweeq database: a solid solution model for Fe-chloritoid [Vidal *et al*., 1994] and unpublished data concerning Fe-glaucophane and epidote (de Capitani, pers. com.). The first calculations confirm that the D1 metamorphic peak conditions previously estimated with Thermocalc yield similar values (15 Kb - 500°C) with a modified Tweeq.

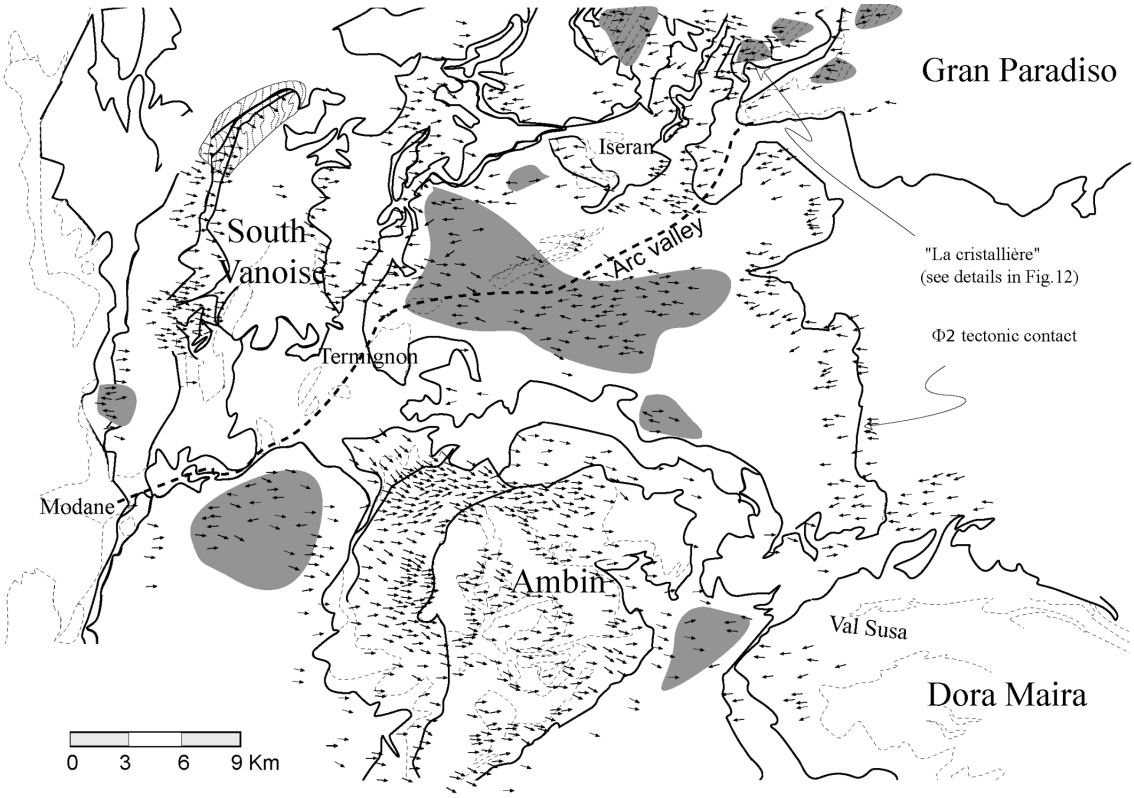

FIG. 9. – Map of D2 stretching lineations (east– and west-directed) observed in the Graies Alps [after Ganne *et al.*, 2006, modified]. A partitioning of the shear deformation can be observed at the scale of the map: (1) in the external part of the Briançonnais domes (Ambin and South Vanoise), east-directed shear deformation is dominant. (2) On the western edge of the internal crystalline massifs (Gran Paradiso, Dora Maira), west-directed shear fabrics are dominant. (3) In between these domains, conjugated shear structures are predominantly observed. The grey patches indicate the area where conjugated shear bands have been observed on single outcrops. In a very general way, simple shear is dominant in the vicinity of the large scale Φ2 tectonic contacts wrapping the basement domes; pure shear is dominant in between these major tectonic contacts (thick, black lines). In the highly sheared areas (in grey), an inversion of the direction of shear could have occurred, leading to the extrusion of material at the footwall of kilometric-scale shear zones (see text for further details).

FIG. 9. – *Carte des linéations d'étirement D2 à l'échelle des Alpes Graies méridionales. Ces linéations sont associées aux plans de cisaillement à vergence Est et Ouest. A l'échelle de la carte, un partitionnement de la déformation cisaillante se dessine :* (1) *à la bordure tectonisée des dômes briançonnais (Ambin, Vanoise Sud), un cisaillement à vergence est domine ;* (2) *à la retombée ouest des Massifs Cristallins Internes (Gran Paradiso, Dora Maira), ce cisaillement est à dominante vers l'ouest ;* (3) *entre ces massifs, les cisaillements présentent des vergences opposées. Les zones ombrées soulignent les domaines où des cisaillements conjugués ont été observés sur un même affleurement. D'une façon plus générale : le cisaillement simple domine à proximité des grands contacts tectoniques Φ2 bordants les dômes de socle, le cisaillement pur domine entre ces grands contacts tectoniques (traits noirs épais). Dans les secteurs fortement tectonisés (zone hachurée sombre), un échappement de matière peut également se produire selon des vergences opposées (voir texte pour explications).*

P-T path

As a whole, the results obtained (fig. 7) from these independent methods (Thermocalc and Tweeq) are in good agreement. They suggest a near-isothermal decompression followed by cooling at decreasing pressure. Maximum pressure estimates were obtained using the Grt-Cld-Gln-Czo-Jd-Rt assemblages thought to represent a prograde path corresponding to garnet growth. Maximum P-T conditions are estimated at around 15 Kb and 500°C. Blueschists and greenschists yielded similar P-T estimates. Unexpectedly, some D1 assemblages yielded lower pressure and/or temperature estimates. This discrepancy may indicate either:

– that the selected phases used for the calculation are not in equilibrium;

– that available thermodynamic data are not well-constrained for the considered mineral assemblage, especially for glaucophane;

– that a few HP-mineral assemblages correspond to the last D1 prograde metamorphic stage (it may be the case for samples Ga-51 and Ga-22);

– that the mineral compositions used for the calculation do not record the stable composition at peak pressure because the mineral have been re-equilibrated by diffusion during the retrograde P.T path (it may be the case for samples Ga-40b, Ga-55).

Indeed, petrological observations related to the D1 structures and associated mineral assemblages suggest that the exhumation process could have been initiated at the final stage of D1. Synmetamorph D1 mineral assemblages including chlorite and intermediate phengite (Si^{4+} = 3.35) have been analysed in the S1 fabric of Claréa rocks. Similar results were also obtained for assemblages located in the most external part (latest) of helicitic garnets tails. Thus the near-isothermal decompression, that follows the HP peak, probably took place at the interface between the two main stages of ductile deformation (D1 and D2). Recent studies

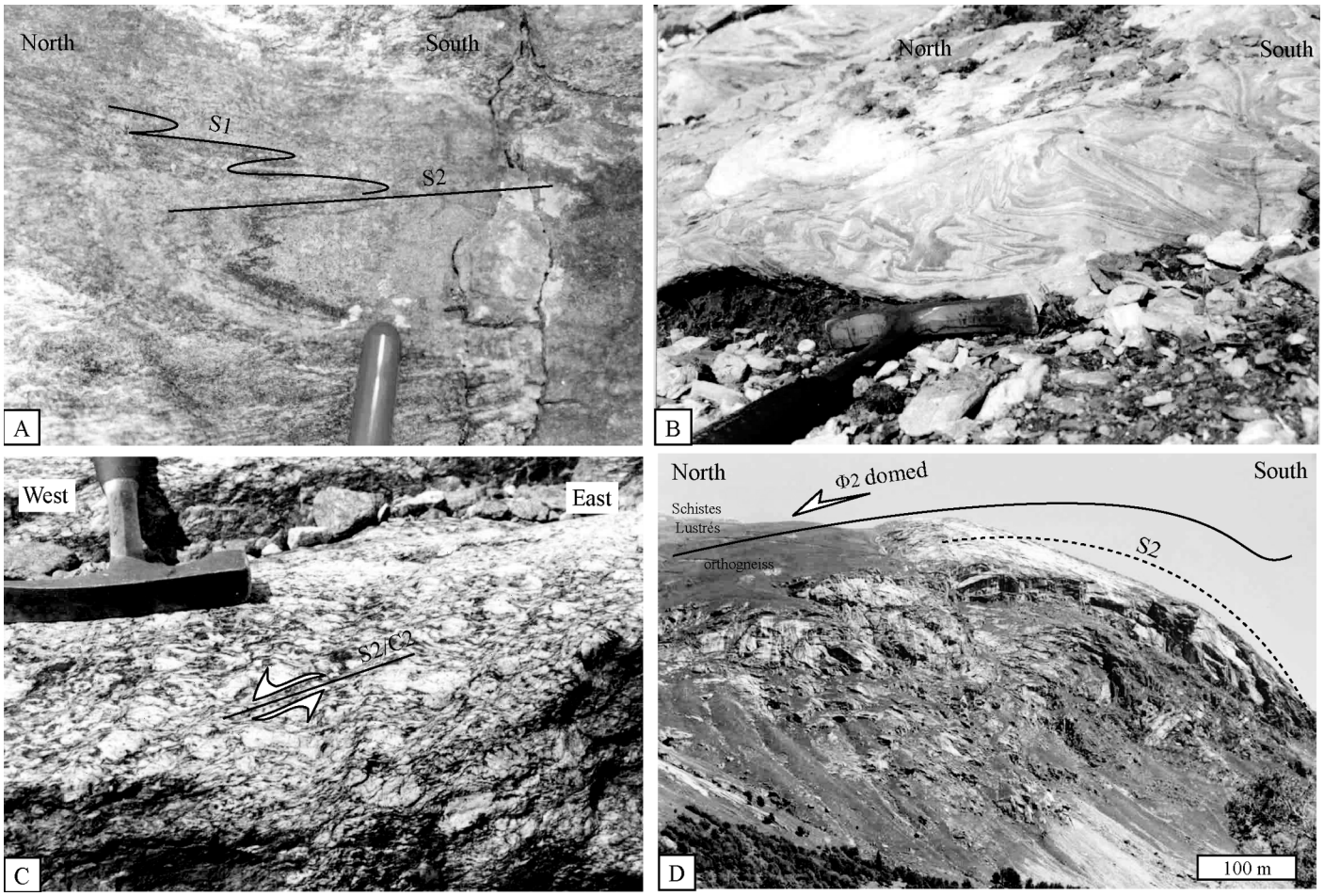

FIG. 10. – D2 shear deformation expressed at the western edge of the Gran Paradiso massif. (A) Early HP-LT S1 fabric (of glaucophane, chloritoid, jadeite, phengite) preserved in a boudin of paragneiss; the S2 planar foliation refolds this early fabric; western edge of the Gran Paradiso massif, Cîme du Caro area. (B) Complex pattern of ductile deformation observed at the bottom of a tectonic calcareous boudin embedded within the paragneisses of the Gran Paradiso massif; east-verging sheath fold, Cîme du Carro area. (C) D2 west-verging shear band observed in an orthogneiss of the Gran Paradiso massif; *Les Evettes* area, western edge of the massif. (D) Φ2 west-verging tectonic contact covering the top of the Gran Paradiso basement. Note the doming of the Φ2 contact by a late D3 fold; "*pli de Bonneval*", western edge of the massif.

FIG. 10. – *Expression de la déformation cisaillante D2 à la bordure ouest du massif du Gran Paradiso.* (A) *Fabrique S1 de HP-BT (glaucophane, chloritoïde, jadéite, phengite) préservée dans un boudin de paragneiss ; la foliation S2 vient transposer cette fabrique S1 (cîme du Caro).* (B) *Plis D2 de vergence est (présentant une géométrie en fourreau) observé au contact entre un boudin calcaire décamétrique et son encaissant de paragneiss (cîme du Carro).* (C) *Shear band D2 de vergence ouest observé dans les orthogneiss du Gran Paradiso (Les Evettes)* (D) *Contact tectonique Φ2 de vergence ouest au sommet du cristallin du Gran Paradiso, déformé par un pli P3 de grande longueur d'onde ("pli de Bonneval").*

support the view that Alpine HP and UHP rocks were not exhumed during a single-step evolution (table I). However, the D2 retrogressive path is the best documented, thanks to TWEEQ, which shows clearly the decrease of both P and T that outlines a fast exhumation. Similarly, the D2 structural evolution is also the best documented from field evidence.

When compared to P-T estimates available for adjacent units – as for example, the "Schistes Lustrés" [Rolland *et al.*, 2000; Agard *et al.,* 2001] – P-T conditions become similar at about 5 Kb, 300ºC which is the stability field determined for D2 (fig. 7). This may be the result of either similar but diachronous P-T paths, or similar and synchronous P-T paths, the onset of the common path corresponding to a tectonic juxtaposition of the two units. The second hypothesis is obviously privileged because microstructural and field studies show that Ambin and "Schistes Lustrés" were strongly deformed together during D2.

Rb-Sr DATING OF PHENGITE

Recent age determinations on Alpine HP minerals [e.g. Rubatto and Gebauer, 1999] and on greenschist facies metamorphic minerals [e.g. Freeman *et al.*, 1997] tend to bracket the time-span of deformation and metamorphism in a very short period, from Upper Eocene to Oligocene, that is in good agreement with stratigraphical evidence [Ellenberger and Raoult, 1979].

A recent study of the Entrelor shear zone, north of the Gran Paradiso dome [Freeman *et al.*, 1997] has shown that the Rb-Sr method on phengite-calcite pairs may be used to obtain deformation ages. If phengite crystallises in a retrograde shear zone, its Si^{4+} content decreases (it is the case at Entrelor and Ambin) and the crystallisation processes occur below the closure temperature of the Rb-Sr system for white mica (ca 550ºC) [e.g. Cliff, 1993]. Radiogenic Sr, especially concentrated in the pre-existing micas, is redistributed between the newly formed micas and low-Rb minerals such as calcite, epidote or feldspar. Assuming that the whole-rock system remained closed and that most micas were recrystallised, the age yielded by the phengite-calcite isochron should correspond to the age of crystallisation of the new phengite. This is especially the case for the most deformed and recrystallised samples where circulating fluids may have enhanced isotopic equilibration processes.

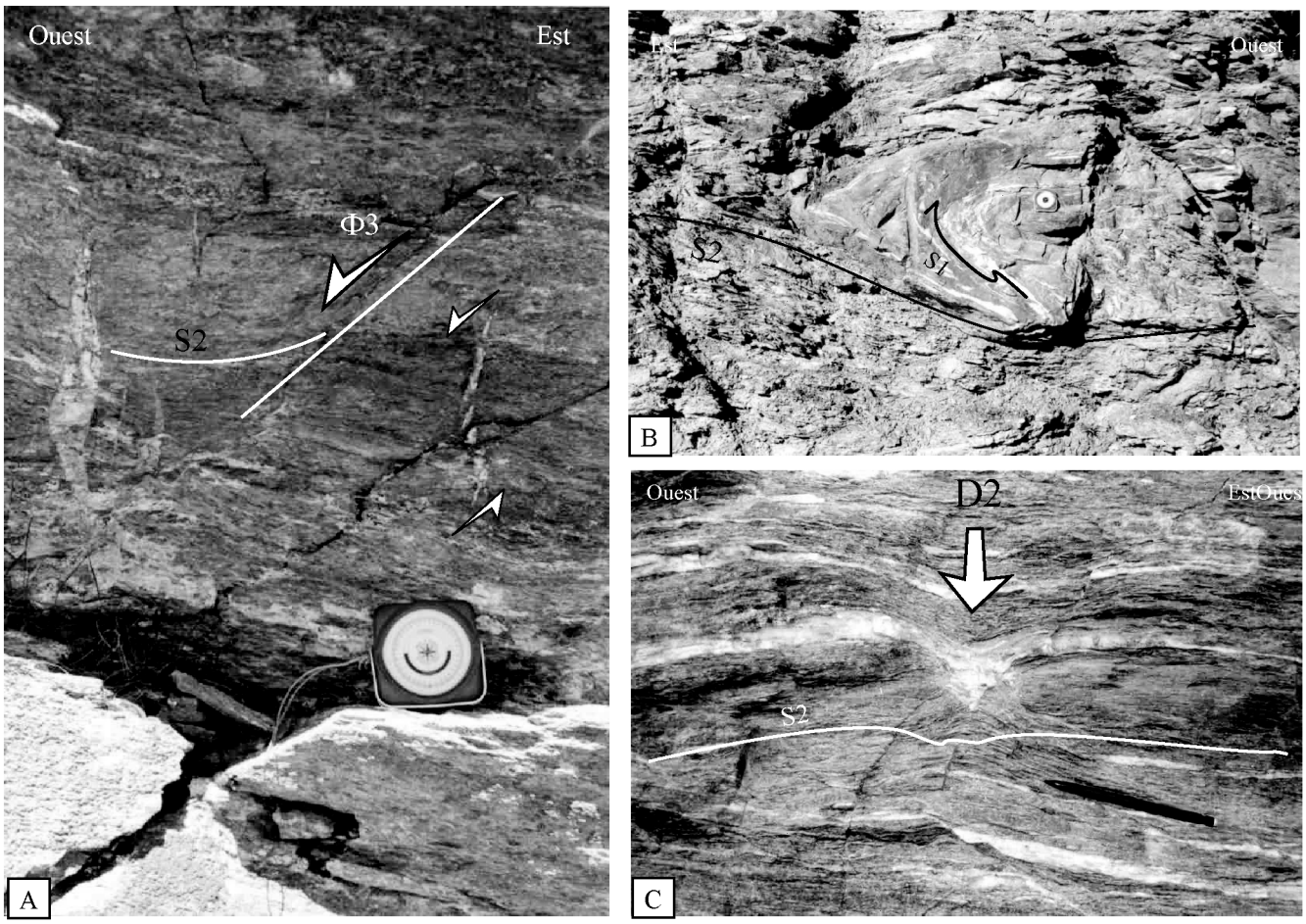

FIG. 11. – Ductile deformation expressed in the Median units of the Schistes Lustrés. (A) D3 deformation: tension gashes and west-verging, brittle-ductile shear bands (Φ3) with steeply dipping appearance cross-cutting through the S2 fabric (west of the Etache valley). (B) F2 fold: an early S1 Alpine fabric, outlined by veins of strongly refolded quartz-calcite, is refolded during D2 ("Fenêtre de Lanslebourg" area). (C) Boudinage of the S2 foliation during D2 shearing. Pure shear is dominant in the sector ("Lanslevillard").
FIG. 11. – *Expression de la déformation ductile dans l'unité médiane des Schistes Lustrés.* (A) *Déformation D3 : fentes de tension et shear bands Φ3) semi-ductiles à vergence ouest recoupant la fabrique planaire S2 (Vallon d'Etache).* (B) *Plis P2 soulignés par des veines de quartz et calcite (fabrique S1 replissée) ("fenêtre de Lanslebourg").* (C) *Boudinage de la fabrique S2 associé au cisaillement D2 ("Lanslevillard").*

Two samples representative of calcite-bearing schists strongly deformed in a shear zone were analysed. Thin section observations indicate that most of the phengitic micas belong to the D3 stage. GA 222 is a coarse-grained calcschist from the uppermost part of the Ambin Group (C unit) where calcite and phengite separated fractions were very pure. Sample ZH 98-32 is a quartz-rich, calcite-bearing phengite schist (C unit) where calcite and phengite fractions were less pure (mixed with quartz). They yielded isochron ages at 34 ± 0,9 Ma (GA 222) and 34 ± 8 Ma (ZH 98 32), identical, within errors, to the main age group obtained by Freeman *et al.* [1997] in the Entrelor shear zone (fig. 8).

DISCUSSION AND CONCLUSIONS

Summary of the post-D1 tectono-metamorphic evolution around the Ambin massif

(1) A major, post-HP deformation affected the Briançonnais, Piemont and Liguria-Piemont units between *Modane, Tignes* and the *Susa valley.* The D2 deformation consists mostly in east- and/or west-directed simple shear from low-grade blueschist facies metamorphism (assemblage of Gln-Cld in the Briançonnais basement and Gln – Lws ± Cld in the Schistes Lustrés complex) to greenschist facies metamorphism (albite-chlorite). There exists, on a regional scale, a partitioning of this retrograde deformation between sectors where simple shear dominates (at the edge of the basement domes) and where pure shear dominates (in between the basement domes). The dominant structures (flat S2 planes and F2 isoclinal folds with curved axis of decametric scale) originated during this D2 shearing deformation.

(2) D2 deformation is superimposed on an early D1 tectonic structure. This structure was characterized by heterogeneous, HP-LT metamorphic conditions. The cores of the Briançonnais domes (Ambin, South Vanoise) were apparently not affected by the D2 shearing deformation and preserve a north-verging, D1 structure [Ganne *et al.,* 2005]. This D1 deformation includes a prograde metamorphic stage, an eclogitic facies peak pressure (garnet-jadeite), and the beginning of retrograde metamorphism [Ganne *et al.*, 2003]. It therefore takes part in the initial stages of the exhumation of the HP-LT Alpine rocks.

(3) The kilometric-scale tectonic contacts Φ2 ± anastomosing, occurred during the D2 deformation. They juxtaposed and deformed the early (D1) HP-LT tectono-metamorphic units during their retrograde metamorphic history. Movement along the Φ2 contacts led to the thinning of the D1 tectonic structures and thus to the exhumation of the HP-LT Alpine rocks [Ganne *et al.,* 2006].

(4) D2 deformation was followed by an overall doming of the crystalline basements and by a down-welling of the Schistes Lustrés units located in between the domes. These large-scale undulations are part of a late, D3 tectonic event, characterised by east- and west-directed movement across the western Alps. D3 may correspond to the final stages of the D2 deformation, in a brittle-ductile tectonic regime.

D1 and D2 structures: thrusts or detachment shear zones?

Data and field observations presented above show that the D1 structures and "nappes" are still difficult to interpret and to fit into a general model. Non-coaxial structures observed in the Claréa rocks suggest that they were probably acquired during the ascent path. However, there are few constraints on the initial geometry of the slices of continental crust formed during D1. We speculated in a brother paper [Ganne *et al.,* 2005] whether the post-Valaisan collision induced some kind of protracted extrusion of slices with an overall N to NW-directed movement.

On the contrary, the scenario is clearer for the D2-D3 combined stages. PT data and structural observations in the Ambin region favour an overall thinning behaviour of the whole Penninic domain during D2 and D3. Such crustal thinning was initiated under low-blueschist facies conditions a short time after the D1 HP metamorphism. In the Schistes Lustrés domain the lower-grade unit (lawsonite-blueschist facies: stability field of carpholite) is lying directly above the Claréa Group (epidote-blueschist facies: stability field of garnet) with an interface comprising the strongly deformed Ambin Group and slices of Mesozoic cover. Thus, although the corresponding metamorphic gap (clearly related to D2) is only a temperature gap, it suggests that the large-scale Φ2 shear zones (fig. 2) may have acted as detachment faults subsequently deformed by open D3 antiforms (e.g. the Ambin dome, fig. 13). Such crustal thinning and extensional behaviour during D2 and presumably D3 constitutes the main conclusion of our work.

Similar large-scale detachment faults, gently dipping toward east or west have been previously described in adjacent units [e.g. Ballèvre *et al.*, 1990; Philippot, 1990; Wheeler and Butler, 1993; Rolland *et al.*, 2000; Agard *et al.,* 2001]. If we accept that these shear zones are synchronous with the Ambin (and Vanoise) Φ2 shear zones, they form a conjugate pattern at regional scale – specifically with the west-verging Gran Paradiso shear zones [Rolland *et al.*, 2000]. They should have played an important role in the unroofing of HP metamorphic rocks exposed at their footwall, as testified by the metamorphic PT path (fig. 13), and probably enhanced the exhumation that was initiated during the still under-constrained D1 extrusion. Such an interpretation is definitely incompatible with the back-folding and back-thrusting concepts classically advocated in most previous works [see Roure *et al.*, 1989 for review] to explain the gently-dipping foliations, often west-dipping, and the apparent east-verging late folds and thrusts that characterise the Penninic domain.

In the particular case of the Briançonnais (and Piemontese?) of central western Alps, it is likely that most structures (D1 and D2) result from the latest subduction-collision event. A larger scale regional view is necessary to justify such an assumption. In the western and central Alps, two southeast-dipping subductions operated successively (and/or partly concurrently) [Stampfli *et al.*, 1998; Schmid and Kissling, 2000], to close the Liguria-Piemont and the Valais oceanic domains. In between the two suture zones, a complex, multistage accretionary wedge has been constituted that comprises both HP "Schistes Lustrés" and Briançonnais terranes but also slices of the Apulian crust (Sesia zone) and of the European crust (Gran Paradiso and

Dora-Maira). The Liguria-Piemont subduction [Le Pichon *et al.*, 1988] that presumably began at ca. 110 Ma culminated with the burial at depth of the Briançonnais units after 45 Ma [Challandes *et al.*, 2002]. Indeed, the assumed age of the youngest subducted sedimentary deposits is Paleocene in age in the Briançonnais domain ("Pralognan" schists of marine origin) [Ellenberger and Raoult, 1979]. During lower Oligocene times (< 34 Ma) the youngest dated sediments of the Valaisan sequence [Bagnoud *et al.*, 1998] – a syntectonic flysch likely deposited while eclogites were formed at depth – suggest that the Valaisan subduction was ending [Challandes *et al.*, 2002]. We are thus dealing with a complex orogenic wedge which was completed by two successive subductions and we do not know for sure whether or not a partial exhumation – alternating collision and extension? – was operating in between. However, the presence of Eocene sediments in the Briançonnais suggests that this domain was only subducted during the youngest subduction event (Valaisan). A similar scenario was previously proposed by Schmid and Kissling [2000]. Thermo-mechanical calculations performed by Bousquet [1998] showed that P-T conditions of 14 Kb, 400°C could be reached close to

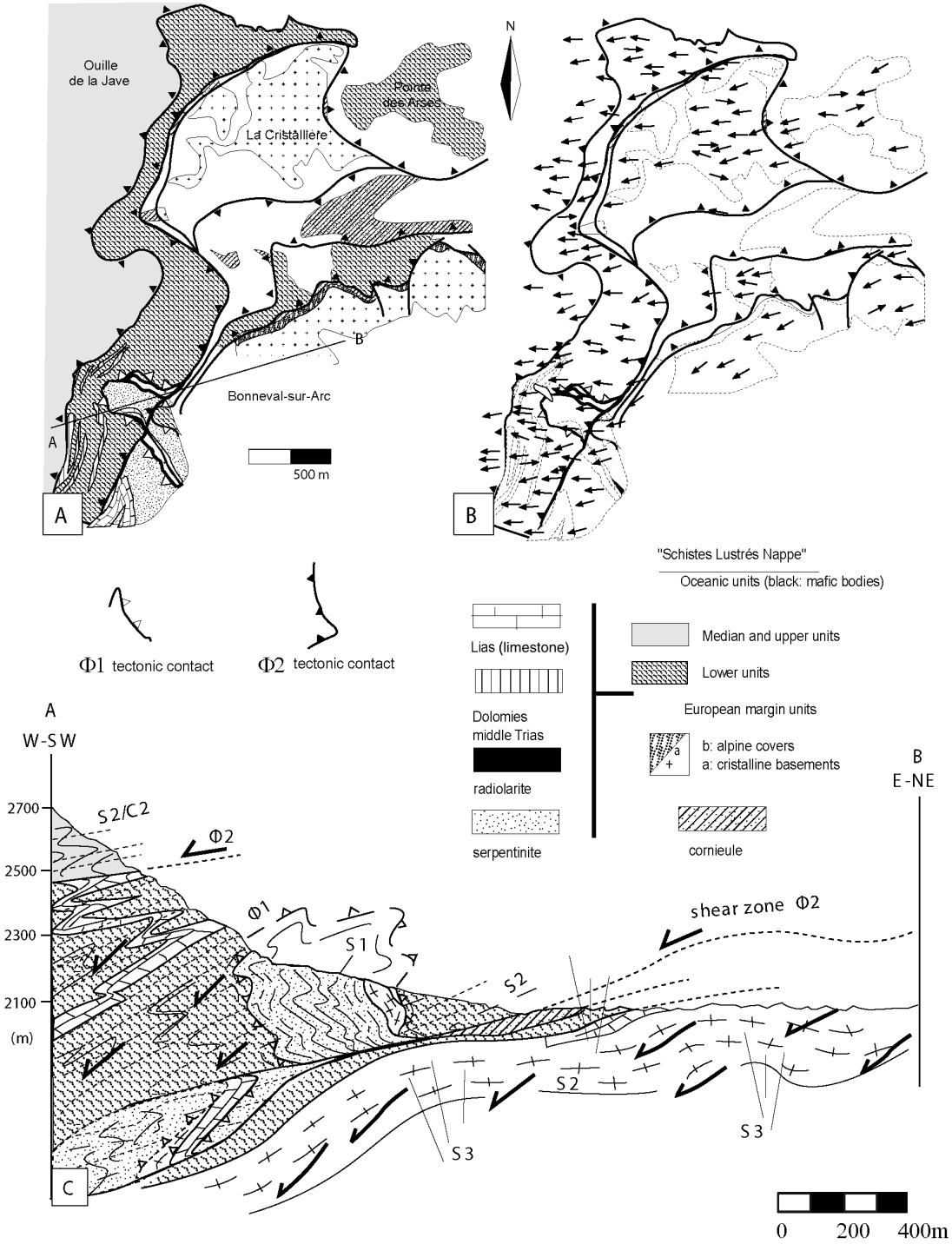

the bottom of a 30-40 km thick accretionary wedge. However, such a setting cannot account for the highest recorded pressure conditions (the deepest known accretionary wedge reaches 40 km; e.g. Olympic mountain, Cascades) [Brandon and Vance, 1992]. This implies that the D1 event, which occurred at higher pressure, was not necessarily linked to the building of the wedge but rather to its subduction and/or exhumation.

Time constraints for the exhumation

Rb-Sr ages of ca. 34 Ma are interpreted as yielding the youngest limit for the last greenschist facies shear zones (D2 ± D3). This result was previously well documented by the study of the Entrelor shear zone further north [Freeman *et al.,* 1997]. Our study, engaged for a comparative test, yielded similar results. Available zircon fission track ages are ranging from 35 to 33 Ma for the internal massifs [Amato *et al.,* 1999; Malusa and Vezzoli, 2006 and references therein]. They suggest that the whole Penninic and Piemontese domains were exhumated up to upper crustal level at that time and that no significant metamorphism occurred subsequently.

The D1 chronology is more difficult to establish. In the Ambin region step-heating argon dating on separated fractions of phengite is in progress. Preliminary results (not quoted here) do not differ from most of available data in other regions of the internal Alps [e.g. Hunziker *et al*., 1992; Barnicoat *et al.,* 1995; Markley *et al.,* 1998; Cartwright and Barnicoat, 2002; Agard *et al*., 2002; Challandes *et al.,* 2002] and suggest ages in the 45-40 Ma range. The dated micas are related to S2 but we cannot preclude from microscopic and microprobe observations micro-scale inter-layering with inherited S1-related phengites. Thus, our study is still unable to explain the discrepancies that occur in many places between strontium and argon ages and especially with U-Pb, Sm-Nd and Lu-Hf ages obtained on UHP rocks [Rubatto, 1998; Duchêne *et al.,* 1997]. In many cases, eclogite ages are in the same range as strontium ages on greenschist facies minerals and younger than argon ages [Ruffet *et al.,* 1995; Arnaud and Kelley, 1995; Scaillet, 1996; Ruffet *et al.,* 1997]. However, the structural and metamorphic study of the Ambin massif suggests some new clues. The sharp change in the deformation regime between D1 and D2 that is not coeval with a similar sharp gap in the metamorphic P-T path suggests that some kind of catastrophic event occurred at ca. 35 Ma. A possible explanation may be found in the slab breakoff hypothesis [Von Blankenburg and Davies, 1995]. In such a case the loss of the "roots": (i) induced a major kinematic change; (ii) enhanced the exhumation process; (iii) was responsible for the very fast exhumation of the last European slices subducted during the closure of the Valaisan trough (Adula, Gran Paradiso, Monte Rosa and Dora Maira) [e.g. Rubatto and Hermann, 2001]; (iv) may explain the temperature peak previously described in several papers [e.g. Platt and Lister, 1985b; Borghi *et al*., 1985-94; Brouwer *et al.,* 2003] – not completely precluded from our data; (v) induced the melting responsible for the Oligocene magmatism (Taveyannaz, Bergell) – [e.g. Boyet *et al*., 2001].

Furthermore, the major change in global plate motions registered in many places [e.g. Dewey *et al.,* 1989] may perhaps be considered as the main culprit for the onset of the Penninic exhumation. But this does not explain why ages older than 35 Ma are preserved in other units: diachronism of D1 (or equivalent) and/or exhumation completed by several successive pulses?

Toward a new alternative exhumation model for the Briançonnais domain

The cartoon presented on figure 13 is a tentative interpretation of what happened in the Ambin region near the times when P-T conditions switched from HP assemblages to greenschist facies. Previously published exhumation models were used to guess a possible geometry and dynamics of the wedge at the time of D1, before 35 Ma, or slightly earlier if argon ages are preferred [Agard *et al*., 2002]. Our observations have shown that we are still unable to know, with reasonable field constraints, what was the geometry of the exhumed slices: foreland verging nappes, foreland and hinterland thrusts, vertical slices or steep fan? This is why we do not propose any starting configuration acquired during

FIG. 12. – The Gran Paradiso – Schistes Lustrés western tectonic contacts: *La Cristallière* area. (A) Geological map [synthesis of previous works: Bertrand, 1968; Robert, 1979; Deville *et al.,* 1992 and unpublished data]. (B) A major, post-HP deformation affected all the Piemont basement and Liguro-Piemont units (Schistes Lustrés) in the western part of the Gran Paradiso massif. This penetrative deformation that we call D2, was operated by west-directed simple shearing in greenschist metamorphic conditions. The black arrows indicate the direction of shearing (stretching and mineral lineations) observed on the S2/C2 shear planes. In the strongly sheared areas observed at the footwall of large-scale Φ2 tectonic contacts, an inversion of the direction of shear can occur (east-verging or conjugated shear fabrics; see text for details). The D2 shear event overprints an early high-grade (HP-LT) tectonic edifice. (C) The boudin of serpentine embedded in the metapelitic units of Schistes Lustrés preserves a steeply-dipping S1 fabric. S1 is parallel to the Φ1 tectonic features outlining the contact with the metapelitic units. We interpreted this boudin as a decametric D1 slice, folded by the D2 shear event. The axial orientation of this fold is roughly N-NW - S-SE. The early high-grade fabrics linked to the slice formation are characterised by HP minerals. Jadeite-bearing S1 fabrics have been analysed in the metagranitic unit include within the boudin of serpentine.

FIG. 12. – *Etude du contact Gran Paradiso – Schistes Lustrés. Secteur La Cristallière.* (A*) Carte géologique des formations [d'après une compilation de travaux antérieurs : Bertrand, 1968 ; Robert, 1979 ; Deville* et al., *1992 et de levés géologiques personnels].* (B) *Une déformation schiste vert D2, opérant par cisaillement simple vers l'ouest, affecte intensément l'ensemble des unités de socles et des unités des Schistes Lustrés présentes sur la retombée sud-ouest du Gran Paradiso. Les flèches noires indiquent les directions de mouvement (linéation d'étirement et linéation minérale) associées aux plans de cisaillement à vergence ouest. Dans les secteurs intensément déformés, le plus souvent à la partie basale des grands cisaillements Φ2 d'extension kilométrique, une inversion des directions de mouvement peut apparaître (cisaillements vers l'est ou cisaillements conjugués : voir texte pour explications). Cette déformation D2, post-HP, se surimpose à un édifice tectonique précoce D1 (la géométrie initiale de cet édifice n'a pu être reconstituée à partir des données cartographiques.* (C) *Le boudin de serpentine emballé dans l'unité métapélitique des Schistes Lustrés préserve une foliation précoce S1 fortement pentée. S1 est parallèle au contact tectonique Φ1 séparant le boudin de l'encaissant métapélitique. Ce boudin correspond selon nous à une écaille tectonique D1 pluri-décamétrique replissée et tronçonnée par la déformation cisaillante D2. L'axe de ce pli présente une direction grossièrement orientée N-NW – S-SE. Les structures précoces associées à cette écaille pluri-décamétrique sont scellées par des minéraux de haute-pression (développement d'une foliation S1 à jadéite dans l'écaille de métagranite associée au boudin de serpentine)*

our D1 stage: we must assume that exhumation is already ongoing. Instead of a poorly constrained ca. 40 Ma-old crustal section, we will try to place ourselves inside the orogenic wedge and to follow the evolution of a small portion of crust, namely the Ambin region, from the end of D1 to the completion of D3. Several previously proposed ideas from the literature were combined for guessing the D1 pattern that is sketched on figure 13A (note that the whole structure may be steeper). They are: – the presence of a lithospheric buttress to allow the preservation of HP assemblages inside the wedge [Chemenda *et al.*, 1997]; – the serpentinite channel concept that allows the ascent of HP assemblages near the bottom of the wedge [Schwartz *et al.*, 2001]; – the "channel flow" concept to guide exhumation along a unique subduction plane [Allemand and Lardeaux, 1997]; – the European affinity of Gran Paradiso, Dora Maira and Monte Rosa [Froitzheim, 2001]; – the underplating (result of the last subduction) of the Valaisan oceanic domain beneath the orogenic wedge [Schmid and Kissling, 2000].

According to the observed finite structural and metamorphic pattern, the successive steps (or stages) may be summarised as follows. On figure 13A, the curved black lines symbolise a forced convection during the early steps of D1. In Ambin, the journey along the P-T path starts in the epidote-blueschists facies (15 Kb, 500ºC, a depth of about

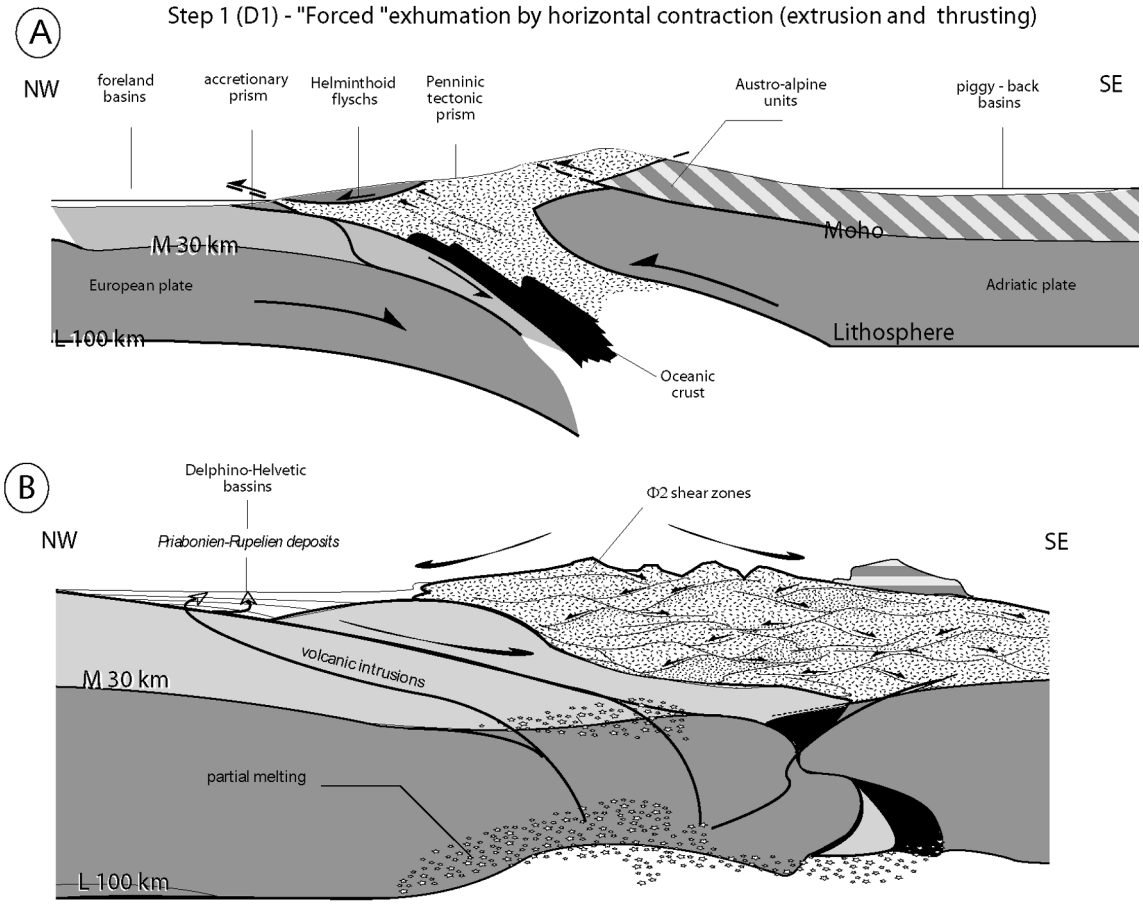

FIG. 13. – Tentative geodynamic model to explain the Penninic HP-rocks exhumation.Two mains steps are summarized on the two sections A and B. Step 1 (D1, section A) corresponds to ca. 35 Ma. At that time the Valaisan trough is still closing, and then a complex orogenic wedge consists in Piemont oceanic rocks, Brianconnais crustal material, Valaisan oceanic rocks ± detached slices of European origin. It is why on the figure the small sedimentary accretionary prism is only formed by the Brianconnais black flysch. The Helminthoid flysch basins are filled up and on their way to be transported. The Penninic HP rocks, a part of which still being in eclogitic conditions, starts their exhumation "journey". Step 2 (D2 and D3, section B) corresponds to ca. 35~32 Ma : the doming process was triggered by the European lithosphere slab break-off and induces extensional motions within the Penninic paleo-orogenic wedge, partial melting and volcanism within the Alpine external domains. According to the Ceriani *et al.* [2001] model, the external Priabonian to Oligocene flysch basin seals the suturing of the Valaisan subduction. Dark arrows = Φ2 shear zones; white stars = partial-melting.

FIG. 13. – *Quel est le moteur de l'exhumation des roches de HP-BT dans le domaine Pennique des Alpes occidentales ?* (A) *Il est vraisemblable que l'enfouissement puis une part très importante de l'exhumation des roches alpines de HP (que nous rattacherons respectivement aux déformations D1 puis D1-D2) se sont produit dans un contexte de subduction ayant impliqué au moins deux domaines océaniques (valaisan et liguro-piémontais). Deux grandes étapes figurées en* (A) *et* (B) *sont à distinguer.* (A) *Un épisode D1 anté-35 Ma où le domaine océanique Valaisan n'est pas encore totalement subduit sous le prisme orogénique pennique.* (B) *Une période charnière (ca. 35~32 Ma) qui voit la fermeture du domaine valaisan et l'émergence d'une déformation cisaillante majeure post-HP (D2). Cette dynamique de subduction (D1-D2) prend fin lors du passage à la collision continentale proprement dite, c'est-à-dire avant 28~30 Ma (contrainte du signal sédimentaire détritique dans les bassins molassiques avec remaniement érosif des galets métamorphisés à HP). Ce changement géodynamique est corroboré par les données traces de fission sur zircon et apatite qui démontrent très clairement pour cette période (20~30 Ma) un très fort ralentissement des vitesses d'exhumation dans les zones penniques. Quelle est l'origine de ce changement géodynamique (D2-D3) : un écaillage brutal de la croûte inférieure européenne bloquant la dynamique de subduction ?, une accrétion plus importante de matériel de marge, 'étouffant' peu à peu cette dynamique ?, la conséquence d'une rupture du panneau lithosphérique en subduction ... ?*

45 km) but microstructural evidence shows that we are already on the retrograde path. When jumping to stage D2, upper crustal conditions are progressively reached, intermediate conditions being suggested by the low blueschists conditions registered during the onset of this stage, the greenschist facies culminating with the main movement along Φ2 shear zones. Thus, exhumation from lower crustal conditions to upper crustal conditions was probably done by thinning (S2 flattening + conjugate D2 shear zones). According to the preference given to U-Pb ages of HP (or UHP) rocks (ca. 35 Ma) or to Argon ages (ca. 40-42 Ma), the D1 to D2 duration may be evaluated at 1 to 8 Ma (30 to 4 mm/yr). The age of the last collapse is only constrained by fission track ages of 30 ± 2 (zircon) and 24 Ma (apatite) from the neighbouring Gran Paradiso massif [Hurford *et al.,* 1989]. If favouring the U-Pb ages of HP and UHP rocks, the D1-D2 evolution must have been catastrophic with very fast exhumation rates [Rubatto and Hermann, 2001]. The orthogonal L1-L2 lineation pattern observed on the field could be the result of such an abrupt change. At a larger scale, the Eocene-Oligocene boundary shows also a complete change in the stress field registered in perialpine sediments. It switches from an Eocene N-S compressional stress field (near-horizontal σ1), to an E-W extension (vertical σ1) during the Oligocene [Bergerat, 1987] responsible for the opening of Oligocene rifts and basins (Rhine, Bresse, Limagne, Provence). Such a sharp change is probably related to a lithosphere-scale event. The break off of the down-going slab [Malavieille *et al.,* 1984; von Blankenburg and Davis, 1995 or Froitzheim *et al.,* 2003] may have initiated a thermo-mechanic rebound of the European lithosphere responsible for a general collapse of the whole orogenic belt (fig. 13B). The Oligocene magmatism, dated at 32-30 Ma, may be a consequence of the slab break-off and the mantle signature of the volcanics emplaced in the External Alps suggests that partial melting of the European lithosphere may be the result of the slab break-off related thermal anomaly [Boyet *et al*., 2000].

Current field-work carried out in neighbouring regions (from the Zone Houillère to the Gran Paradiso) shows that D2 structures are not restricted to Ambin. Our structural observations imply that the D2-related features – both S2 and D2 shear zones – may be considered as a ubiquitous reference datum for understanding the tectonic evolution of the Penninic domain. The last sketch of figure 13B is uncompleted on purpose for its lower boundary: a not scaled sketch showing a possible geometry of the exhumed orogenic wedge, after its collapse, between 34 and 30 Ma, and before the renewal of compression in Miocene times that formed the External Alps.

Acknowledgements. – This study was funded by the GéoFrance3D program (INSU, BRGM, MNERT). Jacques Leterrier (CRPG) is thanked for his help with the Sr isotope analyses. The authors also wish to thank Jacques Malavieille, Stephane Guillot, Laurent Jolivet and Michel Ballèvre for their throughout and extremely constructive reviews, as well as Jean-Marc Lardeaux for his enthusiasm and encouragements.

References

AGARD P., JOLIVET L. & GOFFÉ B. (2001). – Tectonometamorphic evolution of the Schistes Lustrés complex: implications for the exhumation of HP and UHP rocks in the western Alps. – *Bull. Soc. géol. Fr.,* **172**, 5, 617-636.

AGARD P., MONIÉ P., JOLIVET L. & GOFFÉ B. (2002). – Exhumation of the Schistes Lustrés complex: in situ laser probe $^{40}Ar/^{39}Ar$ constraints and implications for the western Alps. – *J. Metam. Geol.*, **20**, 599-618.

ALLEMAND P. & LARDEAUX J.M. (1997). – Strain partitioning and metamorphism in a deformable orogenic wedge: Application to the Alpine belt. – *Tectonophysics*, **280**, 157-169.

ALLENBACH B. (1982). – Géologie de la bordure SW du massif d'Ambin (Alpes occidentales). – Unpublished thesis, Univ. Strasbourg, 138p.

AMATO J.M., JOHSON C.L., BAUMGARTNER L.P. & BEARD B.L. (1999). – Rapid exhumation of the Zermatt-Saas ophiolite deduced from high-precision Sm-Nd and Rb-Sr geochronology. – *Earth Planet. Sci. Lett*., **171**, 425-438.

ARNAUD N.O. & KELLEY S.P. (1995). – Evidence for excess argon during high pressure metamorphism in the Dora Maira massif (western Alps, Italy), using an ultra-violet laser ablation microprobe ^{40}Ar-^{39}Ar technique. – *Contrib. Mineral. Petrol.,* **121**, 1-11.

BAGNOUD A., WERNLI R. & SARTORI M. (1998). – Découverte de foraminifères planctoniques dans la zone de Sion-Courmayeur à Sion. – *Eclogae Geol. Helv.*, **91**, (3), 421-429.

BALLEVRE M., LAGABRIELLE Y. & MERLE O. (1990). – Tertiary normal ductile faulting as a consequence of the lithospheric stacking in the western Alps. – *Mém. Soc. géol. Fr.,* **156**, 227-236.

BARNICOAT A.C., REX D.C., GUISE P.G. & CLIFF R.A. (1995). – The timing of and nature of greenschist facies deformation and metamorphism in the upper Pennine Alps. – *Tectonics*, **14**, 279-293.

BAUDIN T. (1987). – Etude géologique du massif du Ruitor (Alpes franco-italiennes): évolution structurale d'un socle briançonnais. – Unpublished thesis, Univ. Grenoble, 259 p.

BERGERAT F. (1987). – Stress fields in the European platform at the time of Africa-Eurasia collision. – *Tectonics*, **6**, 99-132

BERMAN R.G. (1991). – Thermobarometry using multi-equilibrium calculations: a new technique, with petrological applications. – *Canad. Mineral.*, **29**, 833-855.

BERMAN R.G. & PERKINS E.H. (1987). – GEO-CALC: a software for calculation and display of pressure-temperature-composition phase diagrams. – *Amer. Mineral*., **72**, 861-862.

BERTRAND J.-M. (1968). – Étude structurale du versant occidental massif du Gran Paradiso (Alpes Graies). – *Travaux de Géologie de l'Université de Grenoble,* **44**, 57-87.

BERTRAND J.-M., PIDGEON R.T., LETERRIER J., GUILLOT F., GASQUET D. & GATTIGLIO M. (2000). – SHRIMP and IDTIMS U-Pb zircon ages of the pre-Alpine basement in the Internal Western Alps (Savoy and Piemont). – *Schweiz Mineral. Petrogr. Mitt*., **80**, 225-248.

BOCQUET (DESMONS) J. (1974). – Le socle briançonnais de Vanoise (Savoie): arguments en faveur de son âge antéalpin dans les Alpes française et de son polymétamorphisme. – *C. R. Acad. Sci.*, Paris, D, **278**, 2601-2604.

BORGHI A., CADDOPPI P., PORRO A. & SACCHI R. (1985). – Metamorphism in the north part of the Dora-Maira Massif (Cottian Alps). – *Boll. Mus. Reg. Sci. Nat. Torino*, **3**, 369-380.

BORGHI A., COMPAGNONI R. & SANDRONE R. (1994). – Evoluzione termo-tettonica alpina del settore settentrionale del massicio del Gran Paradiso (Alpi Occidentali). – *Atti Tic. Sci. Terra* (Serie speciale), 1, 137-152.

BORGHI A., GATTIGLIO M., MONDINO F. & ZACCONE G. (1999). – Structural and metamorphic evidence of pre-Alpine basement in the Ambin nappe (Cottian Alps, Italy). – *Mem. Sci. Geol. Padova*, **51**, 205-220.

BOSSE V., BALLÈVRE M. & VIDAL O. (2002). – The garnet isograd in the blueschist-facies metapelites of the île de Groix (Armorican Massif, France): a reccord of ductile thrusting during exhumation. – *J. Petrol.,* **43**, 485-510

BOUSQUET R., OBERHÄNSLI R., GOFFÉ B., JOLIVET L. & VIDAL O. (1998). – High-pressure-low-temperature metamorphism and deformation in the Bündnerschiefer of the Engadine window; implications for the regional evolution of the eastern Central Alps. – *J. Metam. Geol.,* **16**, 657-674.

BOYET M., LAPIERRE H., TARDY M., BOSCH D. & MAURY R. (2001). – Nature des sources des composants andésitiques des Grès du Champsaur et des Grès de Taveyannaz. Implications dans l'évolution des Alpes occidentales au Paléogène. – *Bull. Soc. géol. Fr.*, **172**, 487-501.

BOYET M., LAPIERRE H., TARDY M., BOSCH D. & MAURY R. (2001). – Nature des sources des composants andésitiques des Grès du Champsaur et des Grès de Taveyannaz. Implications dans l'évolution des Alpes occidentales au Paléogène. – *Bull. Soc. géol. Fr.,* **172**, 487-501

BRANDON M.T. & VANCE J.A. (1992). – Tectonic evolution of the Cenozoic Olympic subduction complex, Washington State, as deduced from fission track ages for detrital zircons. – *Amer. J. Sci.,* **292**, 565-636.

BROUWER F. M., VISSERS R. L. M. & LAMB W. M. (2003). – Structure and metamorphism of the Gran Paradiso massif, western Alps, Italy. – *Contrib. Mineral. Petrol.,* **143**, 450-470.

BUSSY F. & CADOPPI P. (1996). – U-Pb zircon dating of granitoids from the Dora-Maira massif (western Italian Alps). – *Schweiz Mineral. Petrogr. Mitt.,* **76**, 217-233.

BUSSY F., SARTORI M. & THELIN P. (1996). – U-Pb zircon dating in the middle Penninic basement of the western Alps (Valais, Switzerland). – *Schweiz Mineral. Petrogr. Mitt.,* **76**, 81-84.

CABY R. (1996). – Low-angle extrusion of high-pressure rocks and the balance between outward and inward displacements of middle Penninic units in the western Alps. – *Eclogae Geol. Helv.,* **89**, (1), 229-267.

CARON J.M. (1977). – Lithostratigraphie et tectonique des schistes lustrés des Alpes cottiennes septentrionales et en Corse orientale (France et Italie). – Unpublished thesis, Univ. Strasbourg. – Mémoire n°**48**, Sciences géologique, 326p.

CARTWRIGHT I. & BARNICOAT A.C. (2002). – Petrology, geochronology, and tectonics of shear zones in the Zermatt-Saas and Combin zone of the western Alps. – *J. Metamorphic Geol.,* **20**, 263-281.

CELMAS A.G. (1982). – Domainal and fabric heterogeneities in the Cap de Creus quartz mylonites. – *J. Struct. Geol.,* **4**, 443-455.

CERIANI S., FÜGENSCHUH B. & SCHMID S.M. (2001). – Multi-stage thrusting at the "Penninic Front" in the western Alps between Mont Blanc and Pelvoux massifs. – *Int. J. Earth Sci. Aug*, **90**, 685-702.

CHALLANDES N., MARQUER D. & VILLA I. (2002). – Dating the evolution of C-S microstructures: a combined ^{40}Ar-^{39}Ar step-heating and UV laserprobe analysis of the Alpine Roffna shear-zone. – *Chem. Geol.,* **14125**, 1-17.

CHALOT-PRAT F., GANNE J. & LOMBARD A. (2003). – No significant element transfer from the oceanic plate to the mantle wedge during subduction and exhumation of the Tethys lithosphere (western Alps). – *Lithos*, **69**, 69-103.

CHEMENDA A.I., MATTAUER M. & BOKUN A.N. (1996). – Continental subduction and a mechanism of high-pressure metamorphic rocks: new modelling and field data from Oman. – *Earth Planet. Sci. Lett.,* **143**, 173-182.

CHEMENDA A.I., MATTE P. & SOKOLOV V. (1997). – A model of Paleozoic obduction and exhumation of high-pressure/low-temperature rocks in the southern Urals. – *Tectonophysics*, **276**, 217-227.

CHOPIN C. (1981). – Mise en évidence d'une discontinuité de métamorphisme alpin entre le massif du Grand Paradis et sa couverture allochtone (Alpes occidentales françaises). – *Bull. Soc. géol. Fr.,* **XXIII**, (7), 297-301.

CLIFF R.A., BARNICOAT A.C. & INGER S. (1998). – Early Tertiary eclogite facies metamorphism in the Monviso ophiolite. – *J. Metam. Geol.,* **16**, 447-455.

CLOOS M. (1982). – Flow melanges: numerical modelling and geochronologic constraints on their origin in the Franciscan subduction complex, California. – *Geol. Soc. Amer. Bull.,* **93**, 330-345.

DESMONS J., COMPAGNONI R., CORTESOGNO L., FREY M. & GAGGERO L. (1999). – Pre-Alpine metamorphism of the Internal zones of the western Alps. – *Schweiz Mineral. Petrogr. Mitt*., **79**, 23-39.

DEVILLE E. (1987). – Etude géologique en vanoise orientale (Alpes occidentales française, Savoie). De la naissance à la structuration d'un secteur de la paléo-marge européenne et de l'océan tethysien: aspects stratigraphiques, pétrographiques et tectoniques. – Unpublished Thesis, Univ. Savoie, 297 P.

DEVILLE E., FUDRAL S., LAGABRIELLE Y., MARTHALER M. & SARTORI M. (1992). – From oceanic closure to continental collision – A synthesis of the Schistes-Lustrés metamorphic complex of the western Alps. – *Geol. Soc. Amer. Bull*., **104**, 127-139.

DÉTRAZ G. & LOUBAT H. (1984). – Faciès à disthène, staurotide et grenat dans un micaschiste appartenant à l'unité des "Gneiss du Sapey" (Vanoise, Alpes françaises). – *Géol. Alpine*, **60**, 5-12.

DEWEY J. F. & RYAN P. D. (1990). – The Ordovician evolution of the South Mayotrough, western Ireland. – *Tectonics*, **9**, 887-901.

DUCHÊNE S., BLICHERT-TOFT J., LUAIS B., TELOUK P., LARDEAUX J.M. & ALBARÈDE F. (1997). – The Lu-Hf of garnets and the ages of the Alpine high-pressure metamorphism. – *Nature*, **387**, 586-588.

ELLENBERGER F. & RAOULT J.-F. (1979). – Les enseignements géologiques des rochers de la Loze à Pralognan (Massif de la Vanoise, Savoie). – *Trav. Sci. Parc. Nation. Vanoise*, **X**, 147-170.

EVANS B.W. (1990). – Phase relation of epidote-blueschists. – *Lithos*, **25**, 3-23.

FREEMAN S.R., INGER S., BUTLER R.W.H. & CLIFF R.A. (1997). – Dating deformation using Rb-Sr in white mica: greenschist facies deformation ages from the Entrelor shear zone, Italian Alps. – *Tectonics*, **16**, 57-76.

FROITZHEIM N. (2001). – Origin of the Monte Rosa nappe in the Pennine Alps – A new working hypothesis. – *Geol. Soc. Amer. Bull.,* **113**, 604-614.

FROITZHEIM N., PLEUGER J., ROLLER S. & NAGEL T. (2003). – Exhumation of high– and ultrahigh-pressure metamorphic rocks by slab extraction. – *Geology*, **31**, 925-928.

FUDRAL S. (1998). – Etude géologique de la bordure téthysienne dans les Alpes franco-italienne nord-occidentales, de la Doire Ripaire (Italie) à la région de Bourg Saint Maurice (France). – *Géol. Alpine*, Grenoble, *Mem. hors série*, **29**, 306p.

FUDRAL S., DEVILLE E. & MARTHALER M. (1987). – Distinction de trois unités dans les " Schistes Lustrés" compris entre la Vanoise et le Val de Suse (Alpes franco-italiennes septentrionales): aspects lithostratigraphiques, paléogéographiques et géodynamiques. – *C. R. Acad. Sci.,* Paris, **305**, II, 467-472.

FUDRAL S., DEVILLE E., POGNANTE U., GAY M., FREGOLENT G., LORENZONI S., ROBERT D., NICOUD G., BLACK C., JAYKO A., JAILLARD E., BERTRAND J.M., FORNO M.G. & MASSAZZA G. (1994). – Lanslebourg Mont-d'Ambin. Carte géologique de la France à 1: 50 000. – BRGM, Orléans.

FÜGENSCHUH B., LOPRIENO A., CERIANI S. & SCHMID S.M. (1999). – Structural analysis of the Subbrianconnais and Valais units in the area of Moutiers (Savoy, western Alps): paleogeographic and tectonic consequences. – *Int. J. Earth Sci.,* **88**, 201-218.

GANNE J, BUSSY F. & VIDAL O. (2003). – Multi-stage garnet in the internal Briançonnais basements (Ambin and South Vanoise massifs): new petrological constraints on the blueschist-facies metamorphism in the western Alps and tectonic implications. – *J. Petrol*., **44**, 1281-1308.

GANNE J., BERTRAND J.M. & FUDRAL S. (2005). – Folds interference pattern at the top of basement domes and apparent vertical extrusion of HP rocks (Ambin and South Vanoise massifs, western Alps). – *J. Struct. Geol.*, **27**, 553 – 570.

GANNE J., MARQUER D., ROSENBAUM G., BERTRAND J.M. & FUDRAL S. (2006). – Partitioning of deformation within a subduction channel during exhumation of HP-LT rocks: a case study in the western Alps. – *J. Struct. Geol.,* **28**, 1193 – 1207.

GAY M. (1971). – Le massif d'Ambin et son cadre de Schistes lustrés (Alpes franco-italiennes). – Unpublished thesis, Univ. Lyon, 296 p.

GEBAUER D. (1996). –A P-T-t path for an (Ultra?) high-pressure ultramafic/mafic rock association and its felsic country-rocks based on SHRIMP-dating of magmatic and metamorphic zircon domains. Example: Alpe Arami (Central Swiss Alps). *In*: S.H.A. BASU, Ed., Earth processes: reading the isotopic code. – AGU, 307-329.

GEBAUER D., SCHERTL H.P., BRIX M. & SCHREYER W. (1997). – 35 Ma-old ultrahigh-pressure metamorphism and evidence for very rapid exhumation in the Dora Maira Massif, western Alps. – *Lithos*, **41**, 5-24.

GOFFÉ B., SCHWARTZ S., LARDEAUX J.-M. & BOUSQUET R. (2004). – Explanatory notes to the map: metamorphic structure of the western Alps and Ligurian Alps. – *Schweiz Mineral. Petrogr. Mitt*., **149**, 125-144.

HEINRICH H. & ALTHAUS E. (1988). – Experimental determination of the reactions 4 lawsonite + 1 albite = 1 paragonite + 2 quartz + $6H_2O$. – *Neues. Jahr. Mineral. Mon.,* **11**, 516-528.

HOLLAND T.J.B. (1980). – The reaction albite = jadeite + quartz determined experimentally in the range 600-120°C. – *Amer. Mineral.*, **65**, 129-134.

HOLLAND T.J.B. & POWELL R. (1998). – An internally consistent thermodynamic data set for phases of petrological interest. – *J. Metamorphic. Geol.,* **16**, 309-343.

HOLDSWORTH R. E. (1990). – Progressive deformation structures associated with ductile thrusts in the Moine Nappe, Sutherland, N. Scotland. – *J. Struct. Geol.,* **12**, 443–452.

HUNZIKER J.C., DESMONS J. & HURFORD A.J. (1992). – Thirty-two years of geochronological work in the central and western Alps: a review on seven maps. – *Mém. Géol.*, **13**, Lausanne, 59 p.

HURFORD A.J., FLISCH M. & JAGER E. (1989). – Unravelling the thermo-tectonic evolution of the Alps: a contribution from fission-track analysis and mica dating. In: M. COWARD, D. DIETRICH & R. G. PARK, Eds, Alpine tectonic. – *Geol. Soc. Sp. Publ.,* **45**, 369-398.

INGER S., RAMSBOTHAM W., CLIFF R.A. & REX D.C. (1996). – Metamorphic evolution of the Sesia-Lanzo Zone, western Alps: Time constraints from multi-system geochronology. – *Contrib. Mineral. Petrol.,* **126**, 152-168.

KRETZ R. (1983). – Symbol for rock-forming minerals. – *Amer. Mineral.,* **68**, 269-279.

LEAKE B.E. (1978). – Nomenclature of amphiboles. – *Amer. Mineral.*, M. **63**, 1023-1052.

LE BAYON B. & BALLÈVRE M. (2006). – Deformation history of a subducted continental crust (Gran Paradiso, western Alps): continuing crustal shortening during exhumation. – *J. Struct. Geol.*, **28**, 793-815.

LEMOINE M. & DE GRACIANSKY P.C. (1988). – Histoire d'une marge continentale passive: les Alpes occidentales au Mésozoïque. Introduction. – *Bull. Soc. géol. Fr.,* (8), **IV**, 597-600.

LE PICHON L., BERGERAT F. & ROULET M.-J. (1988). – Plate kinematics and tectonics leading to the Alpine belt formation: a nex analysis. – *Geol. Soc. Amer. Spec. Paper.*, **218**, 111-131.

LEPINAY B. (1981). – Etude géologique de la région des Gêts et de Samoens (Ht Savoie): les rapports entre les Préalpes du Chablais (nappe de la brèche et nappe des Gêts) et les unités delphino-helvétiques. – Unpublished thesis, Univ. Paris VI, 214p.

MALAVIEILLE J. (1982). – Etude tectonique et microtectonique de la déformation ductile dans les grands chevauchement crustaux: exemple des Alpes franco-italiennes et de la Corse. – Unpublished thesis, Univ. Montpellier, 508 p.

MALAVIEILLE J. (1984). – Modélisation expérimentale des chevauchements imbriqués: application aux chaînes de montagnes. – *Bull. Soc. géol. Fr.,* (7), **XXVI**, 129-138

MALUSA M.G. & VEZZOLI G. (2006). – Interplay between erosion and tectonics in the western Alps. – *Terra Nova*, **18**, 104-108.

MANCKTELOW N. (1985). – The Simplon line: a major displacement zone in the western Lepontine Alps. – *Eclogae geol. Helv.,* **78**, 73-96.

MARKLEY M.J., TEYSSIER C., COSCA M. A., CABY R., HUNZIKER J. C. & SARTORI M. (1998). – Alpine deformation and $^{40}Ar/^{39}Ar$ geochronology of synkinematic white mica in the Siviez-Michabel Nappe, western Pennine Alps, Switzerland. – *Tectonics*, **17**, 3, 407-425.

MÉNARD G. (1988). – Structure et cinématique d'une chaîne de collision. Les Alpes occidentales et centrales. – Unpublished thesis, Univ. Grenoble, 268p.

MERLE O. & MICHON L. (2001). – The formation of the West European rift: a new model as exemplified by the Massif Central area. – *Bull. Soc. géol. Fr.,* **172**, 213-221.

MICHEL R. (1957). – Les faciès à glaucophane dans le massif d'Ambin (Alpes franco-italiennes). – *C.R. somm. Soc. géol. France*, **VII**, 130-131

MONIÉ P. (1990). – Preservation of Hercynian $^{40}Ar/^{39}Ar$ ages through high-pressure low-temperature Alpine metamorphism in the western Alps. – *Eur. J. Mineral.,* **2**, 343-361.

PARRA T., VIDAL O. & JOLIVET L. (2002a). – P-T path of high-pressure, low-temperature schists on Tinos Island (Cyclades Archipelago, Greece) using chlorite-potassic white mica pairs. – *Lithos*, **63**, 41-66.

PARRA T., VIDAL O. & AGARD P. (2002b). – A thermodynamic model for Fe-Mg dioctahedral K-white micas using data from phase equilibrium experiments and natural pelitic assemblages. – *Contrib. Mineral. Petrol.,* **143**, 706-732.

PASSHIER C.W. & TROUW R.A.J. (1996). – Microtectonics. – Springer-Verlag, Heidelberg, 368 pages, 322 illus.,

PFIFFNER O.A., ELLIS O. & BEAUMONT C. (2000). – Collision tectonics in the Swiss Alps: insight from geodynamic modeling. – *Tectonics*, **19**, 1065-1094.

PHILIPPOT P. (1988). – Déformation et éclogitisation progressives d'une croûte océanique subductée: Le Monviso, Alpes occidentales. Contraintes cinématiques durant la collision alpine. – *Doc. Trav. Centre Géol. Géophys. Montpellier*, **19**, 270 p.

PHILIPPOT P. (1990). – Opposite vergence of nappes and crustal extension in the French-Italian Alps. – *Tectonics*, **9**, 1143-1164.

PLATT J.P. (1993). – Exhumation of high-pressure rocks. A review of concepts and processes. – *Terra Nova*, **5**, 119-133.

PLATT J.P. & LISTER G.S. (1985a). – Structural evolution of a nappe complex, southern Vanoise massif, French Penninic Alps. – *J. Struct. Geol.,* **7**, 145-160.

PLATT J.P. & LISTER G.S. (1985b). – Structural history of high-pressure metamorphic rocks in the southern Vanoise massif, French Alps, and their relation to Alpine tectonic events. – *J. Struct. Geol.,* **7** , 19-35.

POGNANTE U. (1991). – Petrological constraints on the eclogite- and blueschist-facies metamorphism and P-T-t paths in the western Alps. – *J. Metam. Geol.,* **9**, 5-17.

POGNANTE U., CASTELLI D., BOGLIOTTI C. & CALLEGARI E. (1984). – Carattere petrografici e petrochemici di alcuni metagabbri ed ortogneiss tardi-paleozoici del massicio d'Ambin, zona Brianzonese interna (Alpi occidentali). – *Rend. Soc. It. Mineral. Petrol*., **39**, 275-780.

POLINO R., DELA PIERRE F., BORGHI A., CARRARO F., FIORASO G. & GIARDINO M. (1999). – Carta geologica d'Italia alla scala 1: 50,000, foglia Bardonecchia. – Note illustrative, 118p.

QUINQUIS M., AUDREN C., BRUN J.-P. & COBBOLD P.R. (1978). – Intense progresive shear in the Ile de Groix blue-schists and compatibility with subduction or obduction. – *Nature*, **273**, 5657, 43-45.

REDDY S.M., WHEELER J. & CLIFF R.A. (1999). – The geometry and timing of orogenic extension: an example from the western Italian Alps. – *J. Metam. Geol.,* **17**, 573-589.

ROBERT D. (1979). – Contribution à l'étude géologique de la haute vallée de l'Arc, région de Bonneval (Savoie). – Unpublished Thesis, Paris 6, 181 p.

ROLLAND Y., LARDEAUX J.M., GUILLOT S. & NICOLLET C. (2000). – Extension syn-convergence, poinçonnement vertical et unités métamorphiques contratées en bordure ouest du Grand Paradis (Alpes franco-italiennes). – *Geodin. Acta*, **13**, 133-148.

ROURE F., POLINO R. & NICOLICH R. (1989). – Poinçonnement, rétrocharriages et chevauchements post-basculement dans les Alpes occidentales: évolution intra-continentale d'une chaîne de collision. – *C. R. Acad. Sci.,* Paris, **309**, II, 283-290.

RUBATTO D. (1998). – Dating of pre-Alpine magmatism, Jurassic ophiolites and Alpine subductions in the western Alps. – Unpublished PhD thesis, ETH Zurich, 160p.

RUBATTO D. & GEBAUER D. (1999). – Eo/Oligocene (35 Ma) high-pressure metamorphism in the Gornergrat zone (Monte Rosa, western Alps): implications for paleogeography. – *Schweiz Mineral. Petrogr. Mitt.,* **79**, 353-362.

RUBATTO D. & HERMANN J. (2001). – Exhumation as fast as subduction? – *Geology*, **29**, 3-6.

RUFFET G., FERAUD G., BALLEVRE G. & KIENAST J.-R. (1995). – Plateau ages and excess argon in phengites: a $^{40}Ar/^{39}Ar$ laser probe study of Alpine micas (Sesia zone, western Alps, northern Italy). – *Chem. Geol.,* **121**, 327-343.

RUFFET G., GRUAU G., BALLEVRE M., FERAUD G. & PHILIPPOT P. (1997). – Rb-Sr and ^{40}Ar-^{39}Ar laser probe dating of high-pressure phengites from the Sesia zone (western Alps): underscoring of excess argon and new age constraints of the high-pressure metamorphism. – *Chem. Geol.,* **141**, 1-18.

SCAILLET S. (1996). – Excess ^{40}Ar transport scale and mechanism in high-pressure phengites: a case study from an eclogitized metabasite of the Dora-Maira nappe, western Alps. – *Geochim. Cosmochim. Acta*, **56**, 2851-2872.

SCHALTEGGER U. & GEBAUER D. (1999). – Pre-Alpine geochronology of the Central, western and southern Alps. – *Schweiz Mineral. Petrogr. Mitt.,* **79**, 79-87.

SCHMID S.M. & KISSLING E. (2000). – The arc of the western Alps in the light of geophysical data on deep crustal structure. – *Tectonics*, **19**, 62-85.

SCHWARTZ S., LARDEAUX J.M., GUILLOT S. & TRICART P. (2000). – Diversité du métamorphism éclogitique dans le massif ophiolitique du Monviso (Alpes occidentales, Italie). – *Geodin. Acta*, **13**, 179-186.

SCHWARTZ S., ALLEMAND P. & GUILLOT S. (2001). – Numerical model of the effect of serpentinites on the exhumation of eclogite rocks: insights from the Monviso ophiolitic massif (western Alps). – *Tectonophysics*, **342**, 193-206.

SEWARD D. & MANCKTELOW N. (1994). – Neogene kinematics of the central and western Alps: evidence from fission-tracks dating. – *Geology*, **22**, 803-806

SPALLA M.I., LARDEAUX J.M., DAL PIAZ G.V., GOSSO G. & MESSIGA B. (1996). – Tectonic significance of Alpine eclogites. – *J. Geodyn.,* **21**, 257-285.

STAMPFLI G.M. (1993). – Le Briançonnais, terrain exotique dans les Alpes ? – *Eclogae Geol. Helv.*, **86**, 1-45.

STAMPFLI G.M., MOSAR J., MARQUER D., BAUDIN T. & BOREL G. (1998). – Subduction and obduction processes in the Swiss Alps. *In*: A. VAUCHEZ & R. MEISSNER, Eds, Continents and their mantle roots. – *Tectonophysics*, **296**, (1-2), 159-204.

TILTON G.R., SCHREYER W. & SCHERTL H.P. (1991). – Pb-Sr-Nd isotopic behavior of deeply subducted crustal rocks from the Dora Maira massif, western Alps, Italy – II: what is the age of the ultra-high-pressure metamorphism? – *Contrib. Mineral. Petrol.,* **108**, 22-33.

TROTET F., JOLIVET L. & VIDAL O. (2001a). – Tectono-metamorphic evolution of Syros and Sifnos Islands (Cyclades, Greece). – *Tectonophysics*, **338**, 179-206.

TROTET F., VIDAL O. & JOLIVET L. (2001b). – Exhumation of Syros and Sifnos metamorphic rocks (Cyclades, Greece). New constraints on the P-T paths. – *Eur. J. Mineral.,* **13**, 901-920.

VIDAL O., THEYE T. & CHOPIN C. (1994). – Experimental study of chloritoïd stability at high-pressure and various fO_2 condition. – *Contrib. Mineral. Petrol.,* **10**, 603-614.

VIDAL O. & PARRA T. (2000). – Exhumation path of high pressure metapelites obtained from local equilibria for chlorite-phengite assemblages. – *Geol. J.,* **35**, (3/4), 139-161.

VIDAL O., PARRA T. & TROTET F. (2001). – A thermodynamic model for Fe-Mg aluminous chlorite using data from phase equilibrium experiments and natural pelitic assemblages in the 100-600ºC, 1-25 Kbar P-T range. – *Amer. J. Sci.,* **301**, 557-592.

VON RAUMER J.F. & NEUBAUER F. (1993). – Late Precambrian and Paleozoic evolution of the Alpine basement – an overview. *In*: J. VON RAUMER AND F. NEUBAUER, Eds, Pre-Mesozoic geology in the Alps. – Springer-Verlag, Berlin, 625-639.

VON BLANCKENBURG F. & DAVIES J.H. (1995). – Slab breakoff: A model for syncollisional magmatism and tectonics in the Alps. – *Tectonics*, **14**, 120-131.

WHEELER J. & BUTLER R.W.H. (1993). – Evidence for extension in the western Alpine orogen – The contact between the oceanic Piemonte and overlying continental Sesia units. – *Earth Planet. Sci. Lett.,* **117**, 457-474.